International Journal of Biological Macromolecules 266 (2024) 131079

Contents lists available at ScienceDirect

International Journal of Biological Macromolecules

journal homepage: www.elsevier.com/locate/ijbiomac

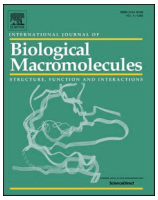

The effect of spent coffee ground (SCG) loading, matrix ratio and biological treatment of SCG on poly(hydroxybutyrate) (PHB)/poly(lactic acid) (PLA) polymer blend

J.Y. Boey [a], U. Kong [a], C.K. Lee [a], G.K. Lim [b], C.W. Oo [b], C.K. Tan [c], C.Y. Ng [d], A.A. Azniwati [a], G. S. Tay [a,*]

[a] School of Industrial Technology, Universiti Sains Malaysia, 11800 USM, Penang, Malaysia
[b] School of Chemical Sciences, Universiti Sains Malaysia, 11800 USM, Penang, Malaysia
[c] PMI Packaging Sdn. Bhd., Taman Perindustrian Senai, 81400 Senai, Johor, Malaysia
[d] CY Enterprise Sdn. Bhd., Taman Perindustrian Murni, 81400 Senai, Johor, Malaysia

ARTICLE INFO

Keywords:
Biological treatment
Spent coffee ground
Biocomposites

ABSTRACT

This study investigates the effects of SCG embedded into biodegradable polymer blends and aimed to formulate and characterise biomass-reinforced biocomposites using spent coffee ground (SCG) as reinforcement in PHB/PLA polymer blend. The effect of SCG filler loading and varying PHB/PLA ratios on the tensile properties and morphological characteristics of the biocomposites were examined. The results indicated that tensile properties reduction could be due to its incompatibility with the PHB/PLA matrixSCG aggregation at 40 wt% content resulted in higher void formation compared to lower content at 10 wt%. A PHB/PLA ratio of 50/50 with SCG loading 20 wt% was chosen for biocomposites with treated SCG. Biological treatment of SCG using *Phanerochaete chrysosporium* CK01 and *Aspergillus niger* DWA8 indicated *P. chrysosporium* CK01 necessitated a higher moisture content for optimum growth and enzyme production, whereas the optimal conditions for enzyme production (50–55 %, *w*/w) differed from those promoting *A. niger* DWA8 growth (40 %, w/w). SEM micrographs highlighted uniform distribution and effective wetting of treated SCG, resulting in improvements of tensile strength and modulus of biocomposites, respectively. The study demonstrated the effectiveness of sustainable fungal treatment in enhancing the interfacial adhesion between treated SCG and the PHB/PLA matrix.

1. Introduction

In the field of materials science and sustainable development, the reliance on non-biodegradable polymers in various industries such as packaging, consumer goods, and automotive parts has sparked major sustainability issues. In response, there is a growing trend to innovate and explore alternative materials that align with the principles of environmental responsibility. Biopolymers, such as poly(lactic acid) (PLA), poly(hydroxyalkanoate) (PHA), polycaprolactone (PCL), and thermoplastic starch, have emerged as viable alternatives to replace fossil fuel-based polymers, offering the potential to reduce greenhouse gas emissions. For instance, PLA derived from renewable resources such as sugarcane and starch, exhibits excellent transparency and mechanical properties similar to conventional polymers like poly(ethylene terephthalate) (PET), polypropylene (PP), and polystyrene (PS) [1,2]. Poly (hydroxyalkanoate) (PHA) is a microbial polyester synthesised by bacteria through sugar and lipid fermentation, offering diverse mechanical properties suitable for applications ranging from packaging films to medical devices [3,4]. Researchers have explored blending PLA and PHA to maximise the properties of each polymer [5–7].

In the pursuit of enhanced material properties and environmental sustainability, natural or lignocellulosic fillers have gained popularity as valuable additions to polymer matrices. These fillers contribute to improved mechanical and physical properties while reducing material density, all in an economically viable and renewable manner [3,8,9]. Spent coffee ground (SCG), a by-product of the coffee industry primarily composed of cellulose and hemicellulose, have drawn interest given their potential value [10]. Despite being considered a pollutant due to its high organic content and the oxygen required for decomposition [11], SCG has previously been used as fertiliser, solid fuels, and animal feed

* Corresponding author.
E-mail address: taygs@usm.my (G.S. Tay).

https://doi.org/10.1016/j.ijbiomac.2024.131079
Received 6 November 2023; Received in revised form 11 March 2024; Accepted 20 March 2024
Available online 26 March 2024

Table 1
Physical and mechanical properties of PLA and PHB [25,26].

Physical properties	Unit	PLA	PHB
Specific Gravity	g/cm^3	1.24	1.24
Melt flow rate, at 210 °C, 2.16 kg	g/10 min	6	8
Clarity		Transparent	
Mechanical properties			
Tensile strength at break	MPa	53	22
Tensile yield strength	MPa	60	
Tensile modulus	GPa	3.5	
Tensile elongation	%	6	350
Notched Izod impact	J/m	16	
Heat distortion temperature	°C	55	

Remarks: Notched Izod Impact refers to impact strength of the material tested using notched Izod method.

supplements [12]. Other than that, SCG also have been implement as material for photothermal material which is a sustainable energy through incorporated into materials such as chitosan and poly(N-isopropylacrylamide) (polyNIPAM) hydrogels [13,14]. On the other hand, there are studies on producing polymer (such as PHA) from SCG through valorization of the SCG, since SCG are rich in lipids, carbohydrates, minerals and proteins [15,16]. Nevertheless, current study has looked into the use of SCG as a filler in polymer composites, offering a sustainable approach to its management. Nguyen & Nguyen [17] have studied the effect of SCG contents on epoxy composites. The results showed that 30 wt% of SCG content is ideal for coffee grounds without phase division on the SCG-epoxy interface. Moustafa et al. (2016) [8] found a significant drop in tensile strength and strain at break with further addition of SCG content (20 wt%) to poly(butylene adipate-*co*-terephthalate) (PBAT) composites.

The incorporation of natural fillers, like SCG, into polymer matrices introduces a challenge stemming from differing polarity and hydrophobicity between the polymer and the filler. This difference affects the adhesion between these two phases, which in turn affects the mechanical performance of the final composites [18]. The mechanical properties of filler-reinforced composites rely on several key factors, including (1) the properties of both the matrix and the filler; (2) the filler content and its distribution within the matrix; and (3) the bond strength between the filler and matrix, which is critical in facilitating load transfer [19–21]. Therefore, researchers have studied various surface treatments to improve interfacial bonding, including chemical, physical, and biological treatments. Despite notable progress in enhancing composites through surface-treated SCG, most studies have concentrated on energy-intensive physical and chemical treatments, often involving large amounts of chemicals and solvents [22–24]. To date, there is limited information on the biological treatment on SCG for the application as filler in polymer matrices. This study investigates the impact of biological treatment of SCG by comparing PHB/PLA biocomposites containing untreated and treated SCG. The investigation takes place in different PHB/PLA ratios and SCG loadings ranging from 10 wt% to 40 wt%. *Phanerochaete chrysosporium* CK01 and *Aspergillus niger* DWA8 are the two different microorganisms used in the biological treatment of SCG to study the change in SCG composition and its subsequent usage as a reinforcing agent. This research aims to contribute to the field of sustainable materials by exploring the potential of SCG as a reinforcing filler in biocomposites and promoting an eco-friendly approach to waste reduction.

2. Experimental

2.1. Materials

Poly(lactic acid) (PLA) (Ingeo 2003D) and poly(hydroxybutyrate) (PHB) (EM10060) in pellet form were obtained from NatureWorks and Ecomann, respectively. The material properties provided by the manufacturers are summarised in Table 1. Spent coffee ground (SCG) was obtained from CY Enterprise Sdn. Bhd. and subjected to oven drying at 70 °C for 24 h to achieve a moisture content of less than 8 %. The dried SCG, with particle sizes ranging from 180 μm to 1 mm, was sieved and stored in a closed container at room temperature (28 ± 2 °C) for subsequent use. Fungal strains *P. chrysosporium* CK01 and *A. niger* DWA8, utilised for biological treatment, were sourced from the culture collection stock of the Bioprocess Technology Division, School of Industrial Technology, USM Penang.

Table 2
Composition of mineral salts [27].

Component	Amount (g/L)
Ammonium nitrate (NH_4NO_3)	5.0
Potassium dihydrogen phosphate (KH_2PO_4)	5.0
Corn steep liquor	2.0
Sodium chloride (NaCl)	1.0
Magnesium sulphate heptahydrate ($MgSO_4{\cdot}7H_2O$)	1.0

2.2. Biological treatment

2.2.1. Fungal cultivation for spore production

Under aseptic conditions, a loop of fungal spores was transferred from the stock culture and streaked onto potato dextrose agar (PDA) slant. The cultures were maintained at room temperature until fully grown. The fully grown slants were sealed with parafilm and preserved at 4 °C with periodic sub-culturing.

2.2.2. Spore counting and inoculum preparation

Spore harvesting was done by introducing a sterile 0.1 % (*w/v*) Tween 80 solution into an agar slant. The spores were collected in suspension by gently scraping the surface of the agar slant using an inoculation loop. The spore concentration was determined using a haemocytometer, and a concentration of 1×10^6 (spores/mL) was used for each fermentation process. The inoculum was prepared by mixing the spore suspensions with the growth medium, which was formulated according to the specifications outlined in Table 2. The pH of the medium was adjusted to 7.0, and sterilisation was carried out at 121 °C for 20 min using an autoclave machine (model: TOMY ES-315, Japan). The medium was allowed to cool to ambient temperature before mixing with spore suspensions.

2.2.3. Solid-state fermentation

SCG was biologically treated using either *P. chrysosporium* CK01 or *A. niger* DWA8 via the solid-state fermentation (SSF) process. SCG was placed in square aluminium trays (16 cm × 16 cm × 5.5 cm), and each tray was covered with aluminium foil before being sterilised at 121 °C for 20 min. Following sterilisation, the trays were allowed to cool to ambient temperature. SSF was conducted with varying moisture content levels, ranging from 40 % to 55 % (*w*/w) at 5 % intervals. Sterile SCG was moistened with autoclaved growth media, inoculated with 20 % (*v/w*) of spore suspension at a concentration of 1×10^6 spores/mL, and the cultures were incubated at room temperature for specific durations. Each experiment was duplicated, and the entire procedure was repeated with different fungal strains for enzyme production.

2.2.4. Enzyme extraction

After completion of the biological treatment, approximately 5 g of treated SCG were separated for glucosamine analysis. The remaining treated SCG was subjected to enzyme extraction by adding 30 mL of 0.1 % (*w/v*) Tween 80 solution to approximately 10 g of the solid substrate. The mixture was maintained at room temperature with occasional manual swirling every 15 min for 1 h. To obtain a crude enzyme solution, the medium was filtered using Whatman No. 1 filter paper. Subsequently, the filtered extract was centrifuged at 8000 rpm for

10 min at 10 °C (model: Kubota 3500). The pellet obtained from the centrifugation was discarded, and the clear supernatant was retained as a source for enzyme analysis. The treated SCG was dried in the oven at 90 °C for 3 days before being incorporated into the biocomposite production process.

2.3. Enzyme activity assays

In this study, three enzymes, carboxymethyl cellulase (CMCase), filter paper activity (FPase), and manganese peroxidase (MnP), were assessed for their activity. All enzyme activity measurements were expressed in units of treated substrate (U/g). All tests were conducted in duplicate, and the results were reported as the mean of the duplicate findings.

2.3.1. Carboxymethyl cellulase (CMCase) activity assay

CMCase activity was determined following the method outlined by Gessesse & Mamo (1999) [28]. A 1 % (w/v) solution of carboxymethyl cellulose (CMC) was prepared in citric-NaOH buffer (50 mM, pH 4.5). One mL of the CMC solution was transferred to a test tube and pre-incubated in a water bath at 55 °C for 5 min. After the pre-incubation, 0.5 mL of appropriately diluted enzyme was added to the same test tube, followed by another incubation at the same temperature for 20 min. The reaction was terminated by adding 2 mL of dinitrosalicylic acid (DNS) reagent and subsequently boiling at 100 °C for 5 min. A control sample was prepared by adding the enzyme after the DNS reagent. The released sugar content was measured spectrophotometrically (model: Hitachi U-1900) at a wavelength of 575 nm, using glucose as the standard.

2.3.2. Filter paper activity (FPase) assay

The FPase activity, expressed in filter paper units (FPU), was determined based on the method developed by Ghose (1987) [29]. One strip of Whatman No. 1 filter paper strip (1 × 6 cm) (Sigma-Aldrich, USA) was added to a solution containing 0.5 mL of culture filtrate and 1.0 mL of 50 mM citric-NaOH buffer (pH 4.5). The mixture was incubated in a water bath at 60 °C for 1 h. The reaction was terminated by adding 3 mL of DNS reagent, followed by boiling for an additional 5 min. After cooling, 20 mL of distilled water was added and thoroughly mixed. A control sample was prepared by adding the enzyme after the DNS reagent. Similar to the CMCase assay, glucose was used as the standard, and the released sugar was measured spectrophotometrically at 540 nm (model: Hitachi U-1900).

2.3.3. Manganese peroxidase (MnP) activity assay

MnP activity was determined by monitoring the oxidation of phenol red in the presence of hydrogen peroxide (H_2O_2), using the modified method of Silva et al. (2014) [30]. The reaction mixture contained 500 μl of enzyme extract, 50 μl of manganese sulfate ($MnSO_4$) (2 mM), 200 μl of bovine serum albumin (BSA) (0.5 % w/v), 100 μl of sodium lactate (0.25 M), 100 μl of phenol red (0.01 % w/v), and 50 μl of H_2O_2 (2 mM) prepared in sodium succinate buffer (0.2 M, pH 4.5). The absorbance was measured at 610 nm using a spectrophotometer (model: Hitachi U-1900) with a reaction time of 5 min at room temperature. The reaction was terminated with 40 μl of sodium hydroxide (NaOH) solution (2 M). Following that, the absorbance was measured for another minute. The control sample was done as described above, but using a heat-inactivated enzyme. The activity was calculated using a molar extinction coefficient value of 4460 mol^{-1} cm^{-1} (Eq. (1)).

$$\text{MnP (U/g)} = \frac{\Delta\text{Abs} \times 10^6}{\varepsilon \times \text{R} \times \tau} \quad (1)$$

where ΔAbs is the difference between the absorbance of the boiled extract and non-boiled extract (i.e., the sample and control) at 0 and 5 min; ε is the molar extinction coefficient of oxidised phenol red at 610 nm = 4460 L mol^{-1} cm^{-1}. R is the aliquot of crude enzyme extract (mL); and τ is the reaction time (min).

2.4. Determination of glucosamine content

The glucosamine content in the fungal mycelia was used as a growth indicator for *A. niger* DWA8 and *P. chrysosporium* CK01 [31]. Approximately 0.1 g of the dried sample obtained from Section 2.2.4. was mixed with 5 mL of 2 M hydrochloric acid (HCl) and boiled for 2 h. The mixture was then cooled and centrifuged (model: Kubota 3500) at 8000 rpm for 10 min at 10 °C. The control sample was prepared as described above, except without boiling. The resulting supernatant (1 mL) was transferred to a new test tube and mixed with 1–2 drops of phenolphthalein in 0.5 % (*v*/v) ethanol. The solution was thoroughly mixed before adding drops of 1 M NaOH solution until a pink colour developed. Neutralisation was carried out by adding 1 % (w/v) KH_2PO_4 drop by drop until the mixture became colourless. This solution, referred to as solution A, was adjusted with distilled water to a final volume of 5 mL.

In another test tube, solution B was prepared by mixing 1 mL of acetyl acetone with 50 mL of 0.5 M sodium carbonate (Na_2CO_3). This solution was freshly prepared and stored in a dark reagent bottle. Next, 3 mL of solution A was mixed with 1 mL of solution B, and the mixture was placed in a boiling water bath for 20 min. After cooling, 6 mL of 95 % ethanol and 1 mL of Erlich's reagent were added to the mixture. The resulting mixture was mixed well, and all tubes were incubated in a water bath at 65 °C for 15 min. After cooling, the absorbance at 530 nm was measured using a spectrophotometer (model: Hitachi U-1900). Erlich's reagent was prepared by dissolving 2.7 g of *p*-dimethylaminobenzaldehyde in 2 mL of absolute ethanol and 2 mL of concentrated HCl, then topped up to 100 mL using concentrated HCl. The standard curve was prepared using glucosamine ranging from 30 to 300 μg/mL with intervals of 30 μg/mL for each point.

2.5. Proximate composition analysis

The proximate composition of both untreated and treated SCG was determined by evaluating the moisture, ash, fat, carbohydrates, crude fiber, and protein content. Standard Association of Official Analytical Chemists (AOAC) methods, as specified in AOAC International (2012) [32], were followed.

2.5.1. Determination of moisture content

The moisture content of a sample was determined by spreading 5 g of the sample over a petri dish that had been dried in the oven. The dish was then dried in an oven at 103 ± 2 °C for 4 h, cooled in a desiccator, and weighed after reaching room temperature. The process was repeated for another 2 h of drying, cooling, and weighing until a constant weight was achieved or a decrease in mass between successive weighing not exceeding 0.5 mg was observed. The moisture content was calculated using Eq. (2) by measuring the sample's weight before and after drying (AOAC 984.25).

$$\text{Moisture content (\%)} = \frac{\text{W}_\text{f} - \text{W}_\text{i}}{\text{W}} \times 100 \quad (2)$$

where W_f is the mass (g) of dried petri dish and undried sample, W_i is the mass (g) of dried petri dish and dried sample, and W is the mass (g) of sample before drying.

2.5.2. Determination of crude fiber content

A 2 g sample was transferred into a round-bottom flask and boiled in 200 mL of 1.25 % H_2SO_4 for 30 min under reflux. The boiled sample was then filtered using filter paper and the residues were returned to the same flask by washing with 200 mL of 1.25 % NaOH. The mixture was boiled for another 30 min under the same conditions before being filtered using weighted filter paper. The filter paper containing the solid

residues was placed in a pre-weighed crucible and dried to a constant weight in the oven at 105 °C. The crucible was weighed once it had completely dried. It was then burned to ashes in a 550 °C furnace. When it had been entirely ashed, it was cooled in a desiccator and weighed. The crude fiber content of the sample was calculated using Eq. (3) (MS 3:1982).

$$\text{Crude fibre } (\%) = \frac{W_1 - W_2 - W_f}{W} \times 100 \quad (3)$$

where W_1 is the mass (g) of empty crucible with dried sample, W_2 is the mass (g) of empty crucible with ashed sample, W_f is the mass (g) of filter paper, and W is the mass (g) of sample before test.

2.5.3. Determination of protein content

Protein content was determined using the standard Kjedahl method according to the in-house method (MS 1194:1999). A 0.5 g sample was mixed with approximately 7.5–8 g of protein catalyst in a Kjedahl flask. The catalyst was prepared using 288 g of anhydrous sodium sulfate (Na_2SO_4), 10.5 g of copper sulfate ($CuSO_4$), and 1.5 g of selenium dioxide (SeO_2). Twelve millilitres of concentrated H_2SO_4 were added to the flask before it was placed in the digestor block for an hour of heating. The digested material was distilled with 40 % NaOH in the Kjedahl distillation apparatus. The solution was heated and distilled until 50 mL was collected in a conical flask. The liberated ammonia (NH_3) was received in 25 mL of 4 % boric acid solution containing bromocressol green and methyl red as indicators. Following that, the green distillate was titrated against 0.1 N H_2SO_4 until it reached the pink end point. A reagent blank was also digested, distilled, and titrated. The protein content was calculated as described in Eqs. (4) and (5).

$$\text{Nitrogen (N)}(\%) = \frac{V \times M \times 14}{W} \times 100 \quad (4)$$

$$\text{Protein } (\%) = N \times 6.25 \quad (5)$$

where V is the volume used for titration, M is the ^{mol}arity of H_2SO_4, and W is the mass (g) of tested sample.

2.5.4. Determination of ash content

Each sample was weighed at 5 g in a pre-weighed porcelain crucible that had been ignited and cooled in a desiccator. The porcelain crucible was ignited in a temperature-controlled furnace at 550 °C for 4 h, or until light grey ash formed. After cooling in the desiccator, it was weighed soon after reaching room temperature. The ash content of the sample was calculated using Eq. (6), in accordance with AOAC 923.03.

$$\text{Ash content } (\%) = \frac{W_2 - W_1}{W} \times 100 \quad (6)$$

where W_1 is the mass (g) of empty crucible, W_2 is the mass (g) of empty crucible with ashed sample, and W is the mass (g) of sample before the test.

2.5.5. Determination of fat content

A dry beaker was added with some anti-bumping granules and weighed as W_1. Each sample of 2 g was weighed (W) and added to the beaker. An amount of 2 mL of concentrated ammonium hydroxide (NH_4OH) was added and mixed thoroughly. After that, 5 mL of concentrated hydrochloric acid (HCl) was added to the same beaker and heated up until the colour changed to brownish. The solution was transferred into a separating funnel with distilled water. Ten millilitres of ethanol were added to the funnel and shaken for 15 s. Another 70 mL of diethyl ether was transferred to the funnel, followed by vigorous shaking for 1 min. The built-up pressure was continuously removed by opening the valve of the inverted funnel with both the stopper and cork held tightly. Seventy millilitres of petroleum ether were added, and the vigorous shaking was repeated for 1 min. The funnel was left for about

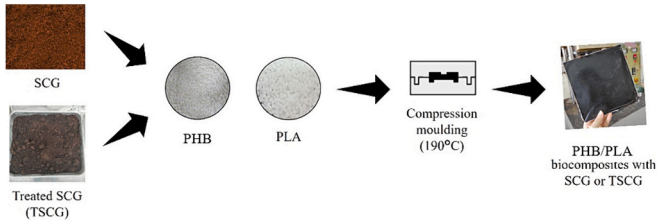

Fig. 1. Schematic preparation of PHB/PLA biocomposites with SCG or treated SCG.

5 min to obtain two layers, i.e., the ether and water layers. The upper layer (ether solution) was decanted into the pre-weighed beaker. The procedure was repeated twice by using 5 mL of ethanol, 70 mL of diethyl ether, and 70 mL of petroleum ether. The solution was decanted into the same beaker used for the first extraction. The solvent was heated on a hot plate in a fume hood until completely evaporated. The beaker with extracted fat was dried in the oven at 100 °C to reach a constant weight. It was cooled in desiccators and weighed (W_2). The fat content of the tested samples was calculated as described in Eq. 7, following the guidelines of AOAC 989.05.

$$\text{Fat content } (\%) = \frac{W_2 - W_1}{W} \times 100 \quad (7)$$

where W_1 is the mass (g) of beaker containing anti-bumping, W_2 is the mass (g) of beaker containing anti-bumping and oil (fat), and W is the mass (g) of tested sample.

2.5.6. Determination of carbohydrate content

The content of available carbohydrate in SCG was determined according to the method specified in the Method of Analysis for Nutrition Labelling, AOAC: 1993 and Food Regulations: 1985. The results were then expressed on a dry weight basis based on Eq. (8).

$$\text{Carbohydrate (g)} = 100 - (\text{moisture} + \text{fat} + \text{protein} + \text{ash} + \text{crude fiber}) \quad (8)$$

2.6. Sample preparation

Before the compounding process, SCG was dried at 70 °C for 24 h. Different weight ratios of untreated SCG and treated SCG were physically pre-mixed with PLA and PHB pellets at pre-determined ratios. A twin-screw extruder (model: LTE-20-40) with screw speed of 75 rpm was used to blend the resins and SCG. The mixture was fed into the extruder at a temperature of 220 °C in the feeding zone, while the other heating zones were maintained at 210 °C as suggested by the data sheet specifications. The molten mixture was extruded at a constant rate and cooled in water at room temperature before being pelletised. The pelletised samples were dried overnight in an oven at 110 °C to prevent moisture absorption.

Table 3
PHB/PLA/SCG blends composition.

SCG loading (wt%)	PHB/PLA ratio				
	100/0	75/25	50/50	25/75	0/100
0	Pure PHB	PHB75/PLA 25	PHB50/PLA 50	PHB25/PLA 75	Pure PLA
10	PHB/ SCG10	PHB75/PLA 25/SCG10	PHB50/PLA 50/SCG10	PHB25/PLA 75/SCG10	PLA/ SCG10
20	PHB/ SCG20	PHB75/PLA 25/SCG20	PHB50/PLA 50/SCG20	PHB25/PLA 75/SCG20	PLA/ SCG20
30	PHB/ SCG30	PHB75/PLA 25/SCG30	PHB50/PLA 50/SCG30	PHB25/PLA 75/SCG30	PLA/ SCG30
40	PHB/ SCG40	PHB75/PLA 25/SCG40	PHB50/PLA 50/SCG40	PHB25/PLA 75/SCG40	PLA/ SCG40

Table 4
PHB/PLA/TSCG blends composition.

Biological treatment	Moisture content (%)	TSCG loading	PHB/PLA ratio
P. chrysosporium CK01	40	TSCG_PC40	PHB/PLA/ TSCGx_PC40
	45	TSCG_PC45	PHB/PLA/ TSCGx_PC45
	50	TSCG_PC50	PHB/PLA/ TSCGx_PC50
	55	TSCG_PC55	PHB/PLA/ TSCGx_PC55
A. niger DWA8	40	TSCG_AN40	PHB/PLA/ TSCGx_AN40
	45	TSCG_AN45	PHB/PLA/ TSCGx_AN45
	50	TSCG_AN50	PHB/PLA/ TSCGx_AN50
	55	TSCG_AN55	PHB/PLA/ TSCGx_AN55

2.6.1. Preparation of PHB/PLA/SCG biocomposites

PHB/PLA/SCG biocomposites were prepared through the compression moulding technique using GOTECH Testing Machines with a model of Hot Press GT-7014-A. The biocomposite pellets were placed into a bronze mould measuring 180 mm × 180 mm × 3 mm. The moulding process consisted of three stages: pre-press, hot press, and cold press. Both the upper and lower mould temperatures were set at 190 °C. During the 12-min pre-press stage, no pressure was applied to ensure complete melting of the pellets. The melted pellets were then compressed at the same temperature for 12 min under 1200 psi pressure for shape formation. Subsequently, the specimens were cooled under the same pressure at room temperature for another 12 min. The biocomposite production procedure is illustrated in Fig. 1. Table 3 presents the weight proportions of the PHB/PLA/SCG blends, with SCG content ranging from 0 to 40 wt%. The nomenclature of the PHB/PLA/SCG biocomposites produced was as follows: PHB/PLA/SCGx for untreated SCG, where x represents the weight percentage of SCG loading. Table 4 provides information on the blend composition of PHB/PLA with treated SCG (TSCG), treated with two fungal species, *P. chrysosporium* CK01 and *A. niger* DWA8. For biological treatment using *P. chrysosporium* CK01 and *A. niger* DWA8, the nomenclature was PHB/PLA/TSCGx_PCy and PHB/PLA/TSCGx_ANy, respectively, where y represents the moisture content employed during fermentation.

2.7. Characterisation

2.7.1. Void content

The void content in biocomposites was determined using the standard provided in ASTM D2734-94 (2003) [33], which provides insights into void occurrence. It was calculated by subtracting the theoretical (T_d) density from the measured (M_d) density of the biocomposites, as shown in Eqs. (9) and (10).

$$T_d = \frac{100}{(\%PLA/\rho PLA) + (\%PHB/\rho PHB) + (\%SCG/\rho SCG} \quad (9)$$

where,

%PLA = weight percent of PLA
ρPLA = density of PLA (g/cm^3)
%PHB = weight percent of PHB
ρPHB = density of PHB (g/cm^3)
%SCG = weight percent of SCG
ρSCG = density of SCG (g/cm^3)

$$\text{Void content } (\%) = \frac{T_d - M_d}{T_d} \times 100 \quad (10)$$

where T_d and M_d are theoretical and measured density (g/cm^3), respectively.

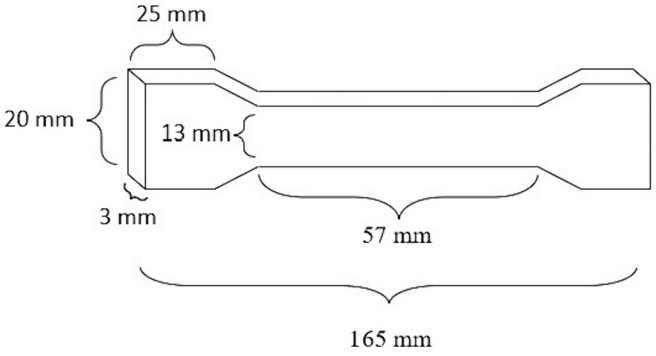

Fig. 2. Dumbbell-shaped sample for tensile test.

2.7.2. Tensile property

Tensile test was carried out using a GOTECH Universal Testing Machine, model GT-TCS-2000, according to the standards outlined in ASTM D638–14 (2014) [34]. A gap of 115 mm between claws was fixed, with a crosshead speed set at 5 mm/min and a load cell of 20 kN. As depicted in Fig. 2, the 3 mm-thick sheets were cut into dumbbell-shaped samples in accordance with ASTM D638 Type I specifications. The strain (elongation) of these samples was measured using a 50-mm extensometer. Tensile properties, including tensile strength, modulus, and strain, were collected and calculated using the instrument's software. Five specimens were tested for each type of biocomposite, and the average values were reported.

2.7.3. Scanning electron microscopy (SEM) analysis

The fractured surfaces of the samples were analysed morphologically using Scanning Electron Microscope (model: EVO-MA10) at an accelerating voltage of 5 kV. Before SEM examination at magnifications of 50× and 100×, the samples were coated with gold (Au) to enhance conductivity.

3. Results and discussion

3.1. Proximate analysis of spent coffee ground

Proximate analysis serves as a useful tool for determining the chemical composition of agricultural biomass. The outcomes of proximate composition analysis, conducted on both untreated (USCG) and treated SCG (TSCG) samples, have been tabulated in Table 5. For a detailed comparison, all values have been expressed as percentages (%), with the results presented on a dry weight basis. Analysis of USCG revealed a composition of 62 % carbohydrate, 11 % crude fiber, 10 % fat, 10 % protein, 5 % moisture, and 2 % ash. After treatment, some alterations in the chemical composition were observed, with an increase in carbohydrate, protein, crude fiber, and ash content, along with a decrease in fat and moisture content.

The study found that all TSCG samples had higher carbohydrate content than USCG, with values ranging from 63.7 % to 71.7 % of the total solids. Among these samples, TSCG_AN45 displayed the most substantial increase in carbohydrate content, reaching 71.7 %, whereas TSCG_AN40 exhibited a relatively lower increase at 63.7 %. This finding is contrary to that of Terefe et al. [35], which reported a decrease in carbohydrate content in maize flour after fermentation with *Lactobacillus plantarum*. This discrepancy might be linked to proportional changes in other components, such as moisture, protein, ash, fat, and crude fiber, resulting from the fermentation process. Carbohydrate content is determined by deducting the values of all other components from 100. Protein content in TSCG samples increased from 10.3 % to 12.9 %, compared to 9.8 % found in the USCG. The increment aligns

Table 5
Proximate analysis of untreated and treated SCG at different moisture content (%, *w*/w).

Parameter	USCG	Moisture content (%, w/w)							
		AN-treated SCG (TSCG_AN)				PC-treated SCG (TSCG_PC)			
		40	45	50	55	40	45	50	55
Carbohydrate	62.3	63.7	71.7	66.6	66.3	65.2	65.5	67.4	65.2
Crude fiber	11.0	12.9	12.0	14.8	12.8	14.3	18.0	14.0	13.8
Fat	10.1	1.9	1.0	3.0	6.5	3.9	2.0	2.1	3.0
Protein	9.8	12.9	11.6	11.9	11.2	11.5	10.3	12.1	12.2
Moisture	5.2	6.4	1.1	1.0	1.0	3.1	1.8	1.8	2.8
Ash	1.7	2.3	2.6	2.6	2.3	2.1	2.4	2.5	3.0

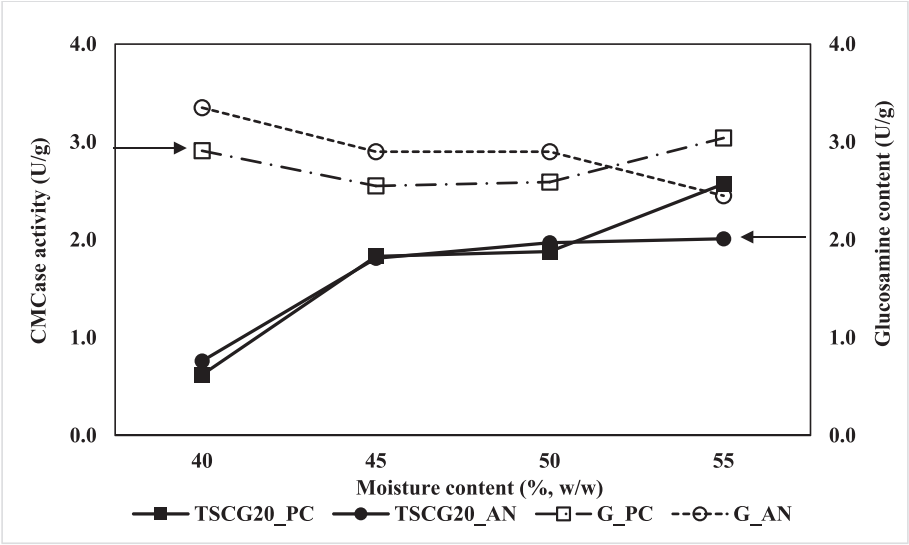

Fig. 3. Effect of moisture content on CMCase enzyme activity produced by *P. chrysosporium* CK01 and *A. niger* DWA8.

with findings in treated coffee pulp [36], sorghum flour [37], and hemp and flax fibers [19]. The enhancement in protein content could be associated with the proteolytic activities of enzymes produced by fungi, releasing peptides and amino acids, resulting in a higher protein proportion in the total mass.

The crude fiber content also experienced an increase in all TSCG samples, with TSCG_PC45 having the highest content at 18 % and TSCG_AN45 having the lowest at 12 %. These results are consistent with those of Olukomaiya et al. (2020) [38], which found an increase in crude fiber content in lupin treated with *Aspergillus sojae* and *Aspergillus ficuum*. It was presumably due to the breakdown of easily digested soluble carbohydrates by the growing fungus, leaving the treated substrate with

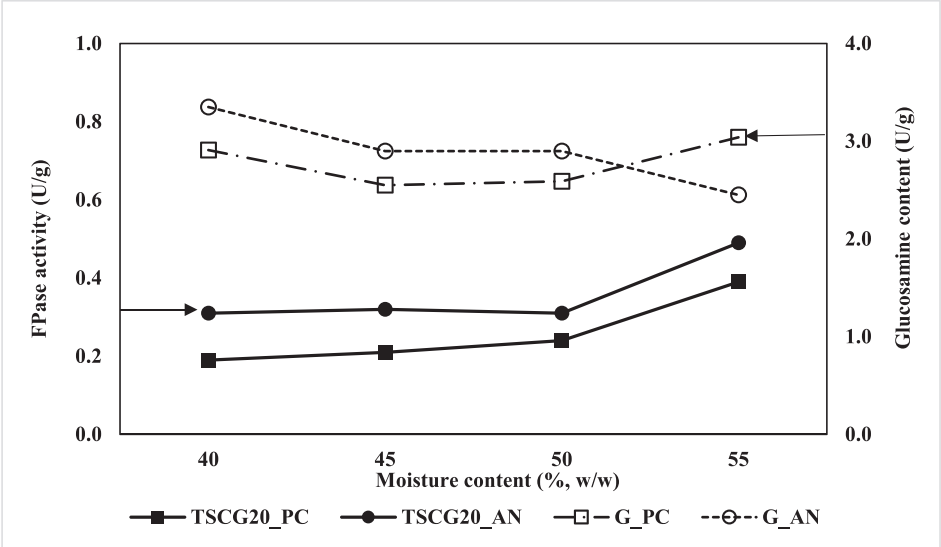

Fig. 4. Effect of moisture content on FPase enzyme activity produced by *P. chrysosporium* CK01 and *A. niger* DWA8.

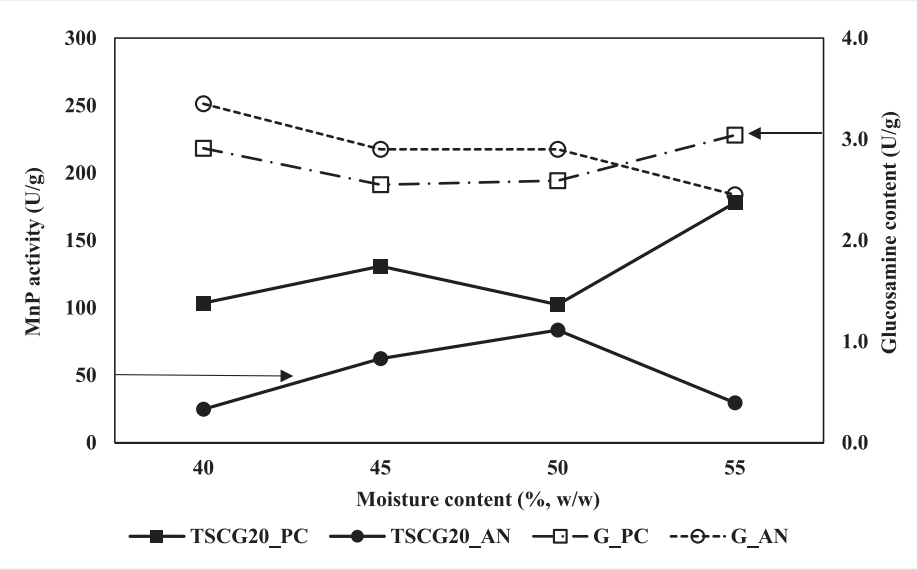

Fig. 5. Effect of moisture content on MnP enzyme activity produced by *P. chrysosporium* CK01 and *A. niger* DWA8.

a higher content of indigestible fiber. Ash content represents the inorganic residue remaining after subjecting the sample to a temperature of 550 °C, ensuring the removal of organic matter. USCG had an ash content of 1.7 %, which increased to a range of 2.1 % to 3.0 % for TSCG. The highest increase (3.0 %) was found in TSCG_PC55, attributed to the loss of organic matter and the accumulation of inorganic matter induced by microorganism activity, resulting in a higher ash content [36,39].

TSCG contained a lower fat content (1–6.5 %) compared to USCG (10.1 %), possibly due to the fungi's enzymatic system secreting lipase to hydrolyse triglycerides into fatty acids and glycerol. This lipid utilisation as an energy source during fermentation could account for fat loss [40]. Particularly, TSCG_AN 45 had the lowest fat content (1.0 %), suggesting sufficient moisture for lipase production, which could also explain its high carbohydrate content after fermentation. The moisture content of TSCG samples varies, with TSCG_AN40 having a slightly higher moisture content (6.4 %) than USCG (5.2 %), while other TSCG samples had a much lower moisture content (1–3.1 %). This variation might be related to the estimated amount of water added to the substrate before fermentation [35]. After fermentation, the moisture content may decrease due to water evaporation during fungal growth, but it remains sufficient for growth and enzyme synthesis [41].

3.2. Enzyme activity analysis

3.2.1. CMCase and FPase enzyme activity

CMCase and FPase are key cellulases responsible for the breakdown of cellulose in substrates into glucose. The effect of moisture variation on CMCase and FPase was studied, and the release of glucosamine content (G_PC and G_AN) representing fungal growth was observed through TSCG (Figs. 3 and 4). SSF setups with moisture contents of 40 %, 45 %, 50 %, and 55 % (*w*/w) were prepared and inoculated with either *P. chrysosporium* CK01 or *A. niger* DWA8 spores. All tested fungi produced cellulolytic enzymes. Moisture content positively influenced CMCase and FPase activities. At 40 % (*w*/w) moisture content, CMCase activity reached 0.62 U/g and 0.76 U/g for *P. chrysosporium* CK01 and *A. niger* DWA8, respectively. These activities increased to 2.57 U/g and 2.01 U/g when moisture content was raised to 55 % (*w*/w). A similar trend was observed with FPase activity, with the highest yields of 0.39 U/g and 0.49 U/g achieved by *P. chrysosporium* CK01 and *A. niger* DWA8, respectively, at a 55 % (w/w) moisture content. It is worth noting that FPase cellulase levels are always lower than CMC levels, which aligns with previous research on fungal fermentation using different substrates. The filter paper substrate used for FPase quantification is known for its resistance to depolymerisation into glucose compared to the CMC substrate used for CMCase quantification [42,43].

The observed results demonstrated that high moisture content, specifically 55 % (w/w), promotes cellulase synthesis in cultures of *P. chrysosporium* CK01 and *A. niger* DWA8, signifying a more effective cellulose degradation process. Lower cellulase production at other moisture levels might be attributed to reduced nutrient solubility and limited substrate swelling, which hinder microbial growth [44]. Previous studies have found that *P. chrysosporium* and *A. niger* can produce cellulase at various moisture content levels, typically falling between 60 % and 80 % [42,45]. In the case of SCG used in this study, 55 % (w/w) moisture content was found to be optimal for maximum cellulase production, largely due to its lower water-absorbing properties. Besides microbial preference, the ideal moisture content can be influenced by substrate characteristics like porosity and particle size [45].

When comparing the two fungal strains, *P. chrysosporium* CK01 grew better and produced more cellulase at 55 % (w/w) moisture content, which corresponded to the higher glucosamine content (G_PC). This was possibly facilitated by the presence of various nutrients in SCG, which enhanced fungal colonisation and enzyme secretion by *P. chrysosporium* CK01 [46]. *A. niger* DWA8 did not follow a similar trend, and it displayed the highest cellulase production at 55 % (w/w) moisture content but lower fungal growth, as indicated by G_AN. This difference could be due to varying moisture requirements for *A. niger* DWA8's growth and enzyme production. The cellulase production by *A. niger* in SSF corresponds with the result obtained by Abdullah & Greetham (2016) [45], which reported the highest activity of 1.302 U/mL at 60 % substrate moisture content.

3.2.2. MnP enzyme activity

MnP is one of the lignin peroxide enzymes involved in the degradation of lignocellulosic biomass. Fig. 5 provides a comparative analysis of MnP production by *P. chrysosporium* CK01 and *A. niger* DWA8 under different moisture contents. *A. niger* DWA8 showed the highest MnP activity at 50 % (w/w) moisture content (83.45 U/g) but decreased to 29.52 U/g at 55 % (w/w) moisture content. On the other hand, *P. chrysosporium* CK01-treated SCG yield the highest activity (177.87 U/g) at 55 % (w/w) moisture content. The two fungal species demonstrated different MnP production profiles, with *P. chrysosporium* CK01 being the best producer. The heightened growth of *P. chrysosporium* CK01 at 55 % (w/w) moisture content, as evidenced by G_PC, contributed to higher

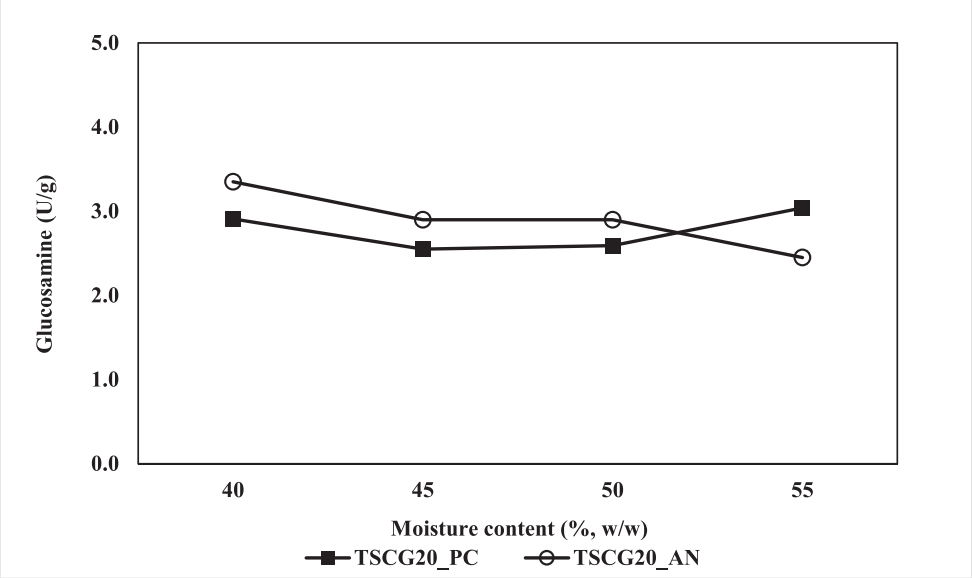

Fig. 6. Effect of moisture content on glucosamine produced by *P. chrysosporium* CK01 and *A. niger* DWA8.

MnP activity. In contrast, *A. niger* DWA8 displayed the lowest glucosamine content (G_AN) and MnP production at 55 % (w/w) moisture content. When SCG was cultured with *A. niger* DWA8 and *P. chrysosporium* CK01, MnP production was higher at 50 % and 55 % (w/w) moisture content, respectively. Low moisture content (40 %, w/w) was found to be unfavourable for MnP synthesis due to limited nutrient solubility [47]. This aligns with previous studies indicating that optimal MnP enzyme activity typically occurs at moisture contents ranging from 50 % to 80 % [30,48]. For instance, Vassilev et al. [49] reported that *P. chrysosporium* achieved maximum MnP activity at 50 % moisture content after 21-day incubation period using a mixture of dry olive and sugar beet wastes. This lower solid-liquid ratio facilitated better mass transfer and enhanced the attachment of fungal mycelium to the substrate particles. The highest MnP activity was reached at 60 % moisture content in *Trametes versicolor* IBL-04 solid-state culture [48]. The optimal moisture content for MnP production varies depending on the substrates used in the SSF process, each having varying water absorption capabilities. Additionally, the moisture requirements of different fungi may also differ, each requiring a specific moisture content for optimal growth.

3.3. Fungal growth

The growth of *P. chrysosporium* CK01 and *A. niger* DWA8 during SSF was assessed by measuring the glucosamine content in SCG substrate, which serves as an indicator of fungal growth. Fig. 6 illustrates the changes in glucosamine content as moisture content varied throughout the fermentation process. Both fungal strains showed different trends in biomass formation. *P. chrysosporium* CK01 and *A. niger* DWA8 achieved greater growth at 55 % and 40 % (w/w) moisture content, respectively. This discrepancy could be explained by the fungi's varying capacities to access and efficiently utilise nutrients under specific SSF conditions. The reduction in *A. niger* DWA8 growth beyond 40 % (w/w) moisture content might be due to reduced substrate porosity and limited oxygen diffusion. Conversely, the decline in fungal growth for *P. chrysosporium* CK01 below 55 % (w/w) moisture content could be due to insufficient water availability, hindering fungal growth and nutrient absorption [50,51].

Moisture content variations influenced enzyme activity in *P. chrysosporium* CK01 during SSF, demonstrating a positive correlation with its growth. *P. chrysosporium* CK01 had the maximum enzyme activity (CMCase, FPase, and MnP) when the moisture content was 55 % (w/w). This indicates that this strain requires higher moisture level for optimal growth and enzyme synthesis. Conversely, *A. niger* DWA8 grew best at 40 % (w/w) substrate moisture. However, at moisture levels of 55 %, 55 %, and 50 % (w/w), it produced the most CMCase, FPase, and MnP enzymes, respectively. This opposite behaviour suggests that enzyme activity in *A. niger* DWA8 is not directly dependent on fungal growth. A similar phenomenon was observed in a study by Carter et al. [52], where the conditions conducive to biomass growth differed from those optimal for phytase synthesis, indicating that enzyme production is not entirely correlated with fungal growth.

Table 6
Measured and theoretical densities of PHB/PLA biocomposites with different PHB/PLA ratio and SCG loading.

PHB/PLA ratio	SCG loading (wt%)	Measured density (M_d) (g/cm^3)	Theoretical density (T_d) (g/cm^3)
100/0	0	1.143	1.240
	10	1.151	1.250
	20	1.143	1.250
	30	1.137	1.250
	40	1.145	1.260
75/25	0	1.144	1.240
	10	1.149	1.250
	20	1.146	1.250
	30	1.143	1.250
	40	1.150	1.260
50/50	0	1.144	1.240
	10	1.151	1.250
	20	1.148	1.250
	30	1.143	1.250
	40	1.151	1.260
25/75	0	1.147	1.240
	10	1.154	1.250
	20	1.150	1.250
	30	1.149	1.250
	40	1.157	1.260
0/100	0	1.150	1.240
	10	1.154	1.250
	20	1.153	1.250
	30	1.151	1.250
	40	1.155	1.260

3.4. Void content and morphology study

The formation of voids during material mixing and consolidation

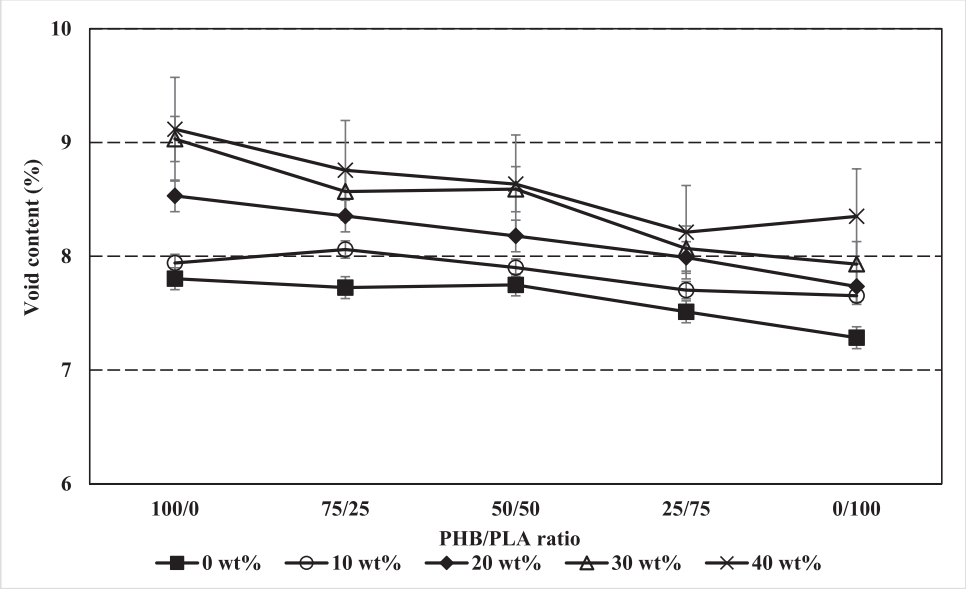

Fig. 7. Effect of PHB/PLA ratio and SCG loading on the void content of the biocomposites.

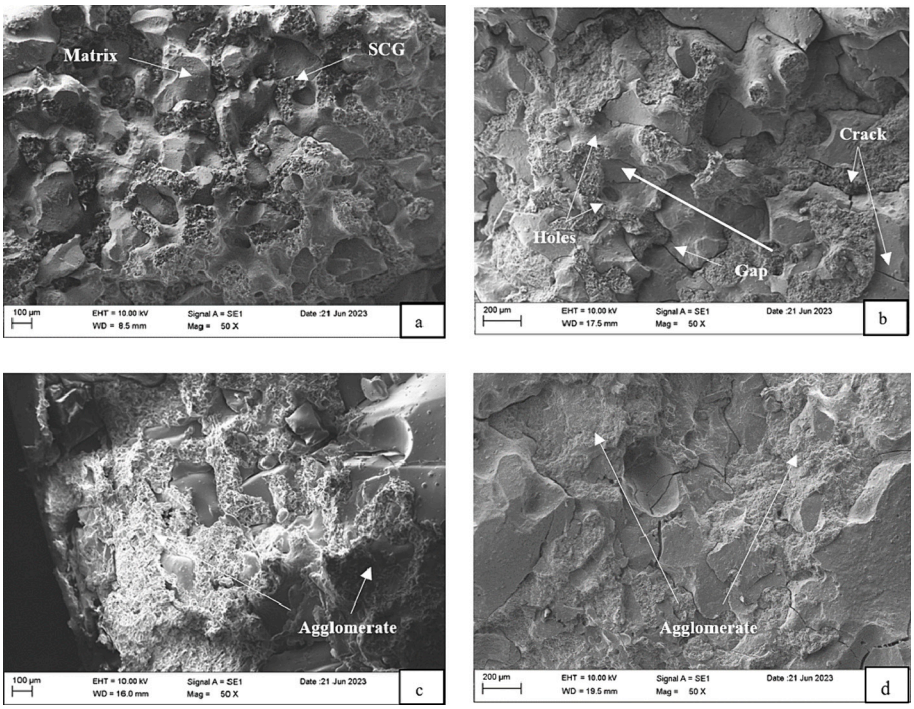

Fig. 8. SEM micrographs (magnification of 50×) of tensile fracture surface for PHB50/PLA50 biocomposites with SCG loading of (a) 10 wt%, (b) 20 wt%, (c) 30 wt%, and (d) 40 wt%.

processes greatly influences the properties of biocomposites. The data on the density and void content of biocomposites are presented in Table 6 and Fig. 7. The data showed that the void content in biocomposites did not significantly differ among different PHB/PLA ratios, with values ranging from 7.28 % to 7.80 %. However, an increase in SCG content within the biocomposites led to a proportionate increase in void content. Notably, biocomposites incorporating 40 wt% SCG exhibited a more pronounced void formation, ranging from 8.2 % to 9.1 %, while those containing 10 wt% SCG showed slightly lower void percentages, ranging from 7.6 % to 8.1 %. These outcomes are in line with the findings published by Sharma et al. (2020) [53] in a work involving fly ash-filled basalt-epoxy composites. This phenomenon might be related to the likelihood of trapped air during biocomposites production, especially when the filler content is high. The variations in cooling rates throughout the processing stages might also contribute to void formation [21]. The measured density are lower than their theoretical counterparts due to voids, as evidenced in the SEM micrographs (Fig. 8 and 9). These voids impede good interfacial adhesion between SCG and the matrix, that showed the incompatibility between SCG and the PHB/PLA matrix. This adversely affect stress transfer at the interphase and compromise the mechanical properties of the biocomposites.

To obtain the desired mechanical characteristics, it is essential to ensure that fillers are uniformly dispersed and fully “wet” within the matrix. Additionally, having strong interfacial adhesion between the

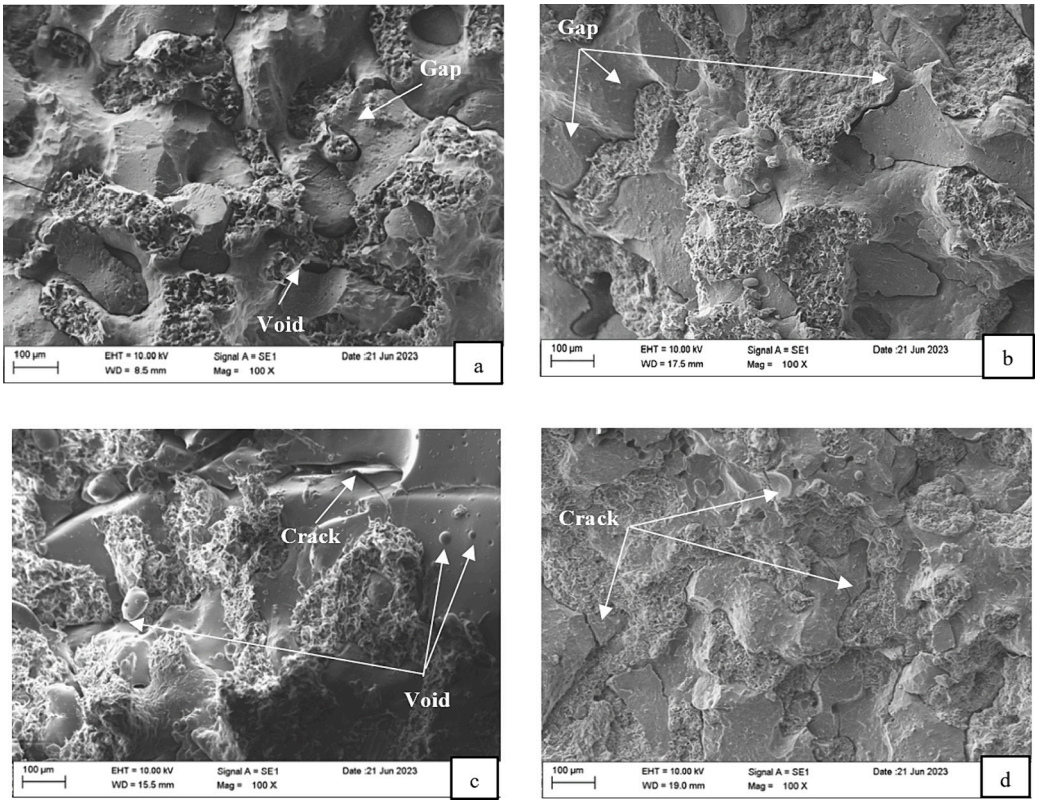

Fig. 9. SEM micrographs (magnification of 100×) of tensile fracture surface for PHB50/PLA50 biocomposites with SCG loading of (a) 10 wt%, (b) 20 wt%, (c) 30 wt %, and (d) 40 wt%.

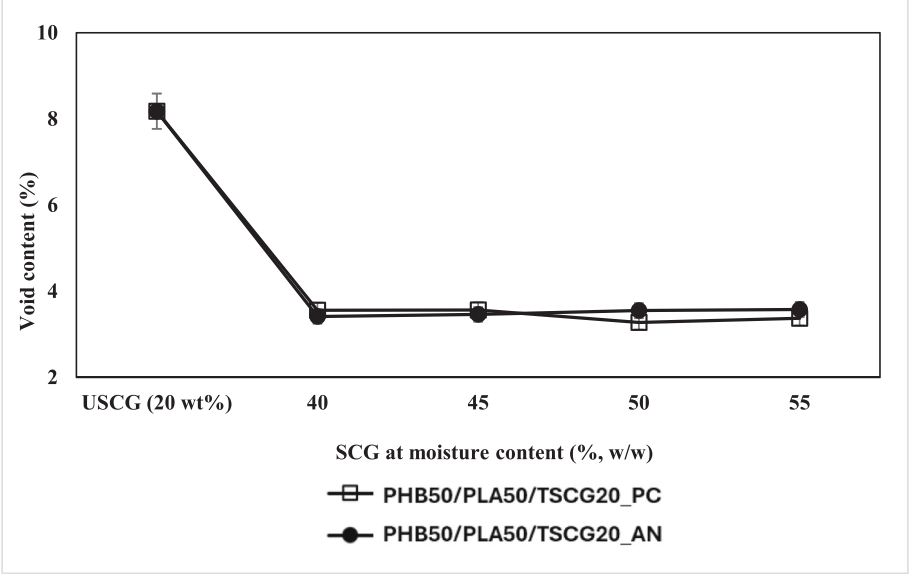

Fig. 10. Void content of PHB/PLA biocomposites with SCG (20 wt%) treated at different moisture contents.

composite components is equally important. The examination of the fractured surfaces of PHB/PLA biocomposites reinforced with USCG was conducted via SEM, with the morphology illustrated in Figs. 8 and 9. These micrographs showed irregular fracture surfaces, largely attributed to the disruptive effect of fillers on matrix continuity. The samples also showed evidence of debonding between the phases in the form of voids, cracks, and gaps between USCG and the matrix at the interfaces. This observation aligns with previous studies, including those by Essabir et al. [22], Xu et al. [54], and Zhuo et al. [55]. The underlying reason for these occurrences could be traced to the inherent poor compatibility between the hydrophilic SCG and the hydrophobic matrix.

The distribution of SCG particles in biocomposites was acceptable when the SCG content was below 20 wt% (Fig. 8a and b). However, when SCG content increased beyond 20 wt%, densely packed and highly aggregated particles appeared, leading to poor interfacial adhesion (Fig. 8c and d). This occurrence signified insufficient and inadequate matrix wetting, leading to reduced stress transfer across the filler-matrix interface [56]. At the same time, biocomposites with 30 and 40 wt% SCG

Table 7
Measured and theoretical densities of PHB50/PLA50 biocomposites with untreated and treated SCG (20 wt%).

PHB50/PLA50 biocomposites with USCG/TSCG (20 wt%)	Measured density (M_d) (g/cm^3)	Theoretical density (T_d) (g/cm^3)
Untreated SCG	1.148	1.250
TSCG_PC40	1.189	1.233
TSCG_PC45	1.182	1.226
TSCG_PC50	1.196	1.236
TSCG_PC55	1.191	1.233
TSCG_AN40	1.210	1.253
TSCG_AN45	1.199	1.242
TSCG_AN50	1.199	1.243
TSCG_AN55	1.198	1.242

presented larger void volumes and sizes compared to those with 10 and 20 wt% SCG. These voids acted as interfacial defects, potentially impacting the mechanical properties of the biocomposites, which was consistent with lower tensile properties observed in the tested samples.

Biocomposites with TSCG had fewer interfacial voids, approximately 3 %, compared to PHB50/PLA50/SCG20 biocomposite, which had 8.2 % voids (Fig. 10). This finding suggests that the PHB/PLA matrix improves the wettability of TSCG, and the removal of non-cellulosic components contributes to better adhesion at the interface. The density of TSCG-reinforced biocomposites was higher than that of USCG-reinforced biocomposites (Table 7), due to the higher density of TSCG and reduced voids. The narrowed gap between TSCG and the PHB/PLA matrix explains the improved interaction, as evidenced in the SEM micrographs (Fig. 11), preventing void formation. This result closely parallels the findings of Vishnu Vardhini et al. (2018) [57], where PP composites developed from alkali and enzymatically treated banana fiber had fewer voids and better fiber-matrix bonding.

SEM micrographs of fracture surfaces of PHB/PLA/TSCG biocomposites showed improvement with TSCG (Fig. 11a-d). TSCG exhibited better dispersion and enhanced homogeneity within the PHB/PLA matrix, signifying that the matrix effectively wetted TSCG, forming stronger interactions between the two components and strengthening the interfacial adhesion [56]. The removal of non-cellulosic components and impurities exposed microfibrils on the surface, rendering it rougher. In addition, the modification in surface roughness was also influenced by the hyphal growth on the SCG surface [58]. By removing hydroxyl groups from non-cellulosic components, fungal treatment increased the hydrophobicity of SCG, giving them a similar character to that of the matrix. This transformation facilitated better mechanical anchorage between the TSCG and the matrix, enhancing tensile properties in TSCG-reinforced PHB/PLA biocomposites. As previously discussed, polymer stress transfer to fillers depends on the interaction between the filler and the polymer, along with the filler's dispersion. Apparently, TSCG particles were embedded well in the matrix, with fewer gaps at the interface, indicating improved interactions when compared to those observed with USCG and the PHB/PLA matrix. These well-bonded particles play a pivotal role in facilitating stress transfer throughout the composite structure [20]. SEM analysis showed that the PHB/PLA matrix and hydrophilic TSCG had a significant compatibilising effect as a result of biological treatment. Similar findings have been reported in the enzymatic treatment of bamboo and banana fibers by Zhuo et al. (2020) [55] and Vishnu Vardhini et al. (2018) [57], respectively.

3.5. *Effect of PHB/PLA ratio and SCG loading on the tensile properties*

3.5.1. *Tensile strength*

The study formulated 25 biocomposites with different combinations of SCG loadings (0–40 wt%) and PHB/PLA ratios. Fig. 12 illustrates the tensile strength of the biocomposites. The results showed that

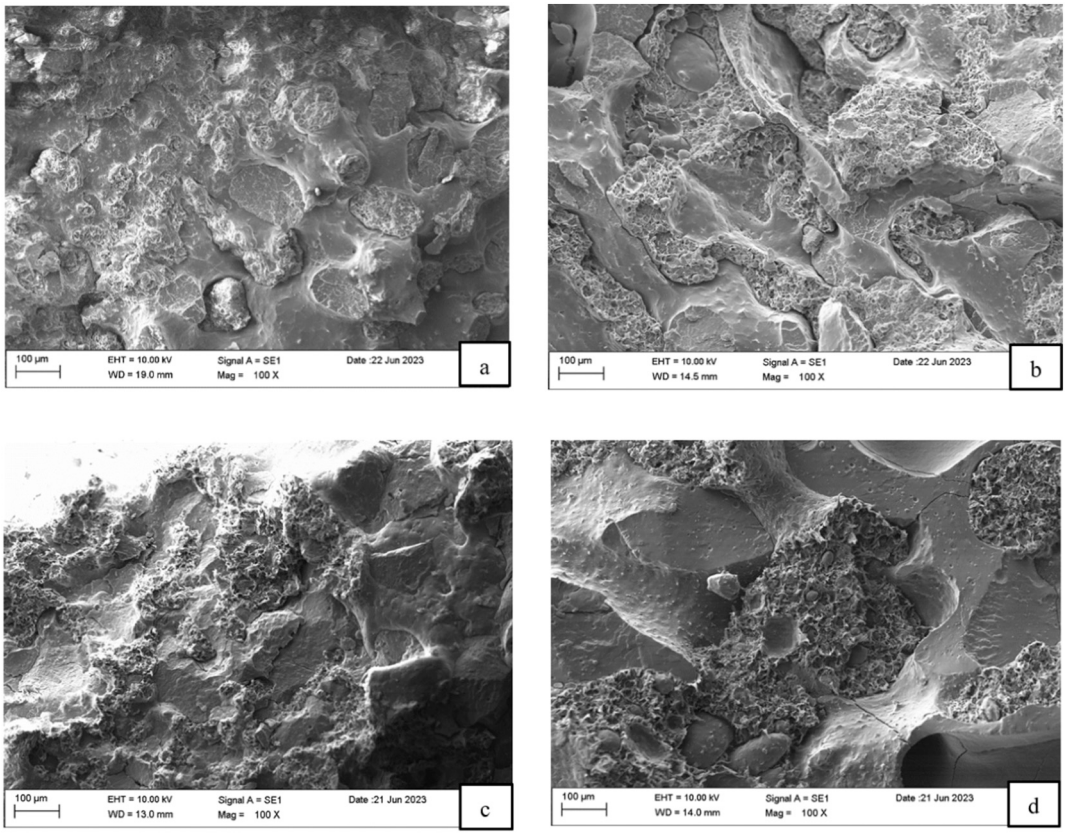

Fig. 11. SEM micrographs (magnification of 100×) of tensile fracture surface for (a) PHB50/PLA50/TSCG20_PC45, (b) PHB50/PLA50/TSCG20_PC55, (c) PHB50/PLA50/TSCG20_AN45, and (d) PHB50/PLA50/TSCG20_AN55 biocomposites.

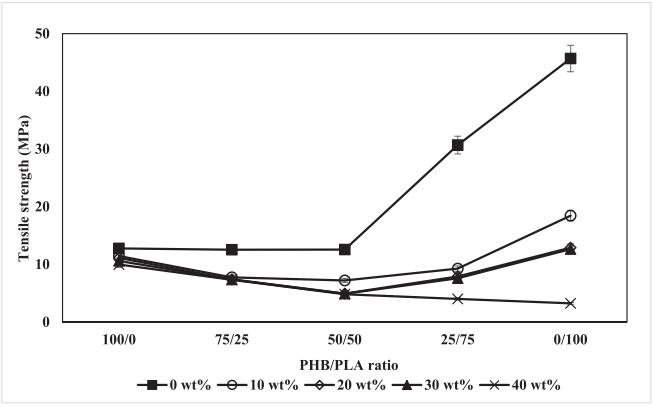

Fig. 12. Tensile strength of PHB/PLA biocomposites with different combination of USCG and PHB/PLA matrix ratio.

biocomposites with higher PLA content showed improved tensile strength, as PLA has a higher tensile strength than PHB, measured at 45.68 MPa compared to 12.76 MPa for PHB. This observation aligns with the research of Aydemir & Gardner [59], indicating enhanced mechanical properties in neat PHB with greater PLA content.

The introduction of SCG in biocomposites led to a reduction in tensile strength. The most significant cases happened at PHB25/PLA75 and pure PLA, the tensile strength dropped from around 30 MPa and 45.68 MPA to below 10 MPa and 20 MPa respectively for all cases of the composites incorporated with SCG. The tensile strength ranged from 7.20 to 18.43 MPa for biocomposites containing 10 wt% SCG and from 3.23 to 9.96 MPa for those loaded with 40 wt% SCG. This behaviour was driven by a combination of filler addition, inherent differences between the matrix and SCG, and the absence of surface treatment. There was inadequate stress transmission from the PHB/PLA matrix to the SCG filler due to the absence of an effective filler-matrix interface. This statement was supported by the SEM micrograph (Fig. 8), which illustrates the formation of gaps at the interfaces. The possibility of SCG agglomeration may also contribute to the decline in tensile strength at higher SCG concentrations. The matrix's ability to completely "wet" all SCG particles in its molten state diminishes, leading to filler-filler interactions predominating over filler-matrix interactions, potentially forming voids at the interface. This compromises the interface bond strength and stress transfer efficiency, negating the strengthening effects [60]. This result is in accord with several studies indicating that excess filler content could affect the resulting composites [10,61,62].

The initial phase of this study found that high SCG content in the formulations caused agglomeration and non-uniform bonding between the filler and the matrix. This, in turn, had an adverse impact on the tensile properties of the resulting biocomposites. Additionally, increased SCG content introduced more voids, further compromising load transmission within the biocomposites.

To address the ductility and brittleness characteristics of the biopolymer blend, the subsequent experiment focused on a PHB/PLA ratio of 50/50. In this ratio, PHB increased the blend's crystallinity, while PLA increased the stiffness. Increasing the PLA ratio within the blend could enhance the mechanical properties of the biocomposites. Hence, the PHB/PLA ratio of 50/50 was chosen for producing biocomposites with treated SCG (TSCG). This choice was motivated by the objective of assessing whether these biocomposites exhibited superior mechanical properties in comparison to those with a higher proportion of PLA within the blend. TSCG was incorporated at a loading of 20 wt% for reinforcement. This loading was chosen with consideration for processability since higher loadings (ranging from 30 to 40 wt%) tend to cause extruder blockages and material flow difficulties during compounding process. It is worth noting that biocomposites with a high filler content may experience agglomeration issues, leading to localised stress concentration points, non-homogeneous dispersion, and reduced load-bearing ability [60,63].

SCG was biologically treated as an approach to improve its compatibility with the PHB/PLA matrix. As depicted in Fig. 13, the tensile strength of PHB/PLA biocomposites with SCG treated by *P. chrysosporium* CK01 (PHB50/PLA50/TSCG20_PC) and *A. niger* DWA8 (PHB50/PLA50/TSCG20_AN), was evaluated alongside biocomposites incorporating untreated SCG (PHB50/PLA50/SCG20). The results revealed that biocomposites employing treated SCG (TSCG) demonstrated enhanced properties compared to their counterparts utilising untreated SCG (PHB50/PLA50/SCG20). The most substantial improvement in tensile strength was observed in the PHB50/PLA50/TSCG20_PC45 biocomposite, with a tensile strength of 8.44 MPa, representing a remarkable 72 % increase compared to the biocomposite with USCG (PHB50/PLA50/SCG20), with a tensile strength of 4.92 MPa. The PHB50/PLA50/TSCG20_AN50 biocomposite exhibited a 64 % increase, with a tensile strength of 8.06 MPa. The smallest increment of 3 % was observed in the PHB50/PLA50/TSCG20_AN55 biocomposite, reaching a value of 5.08 MPa.

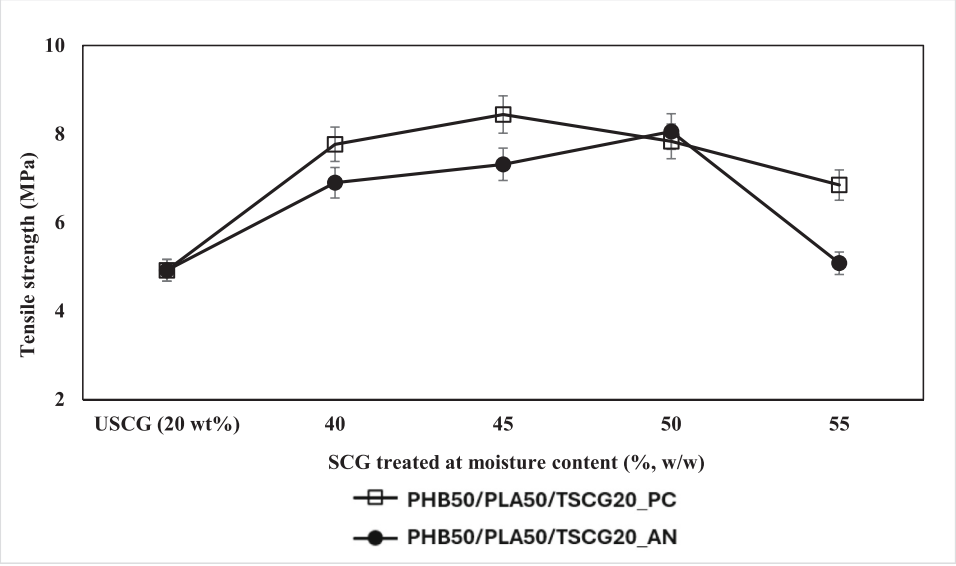

Fig. 13. Tensile strength of PHB/PLA biocomposites with SCG treated at different moisture contents.

Fig. 14. SCG surface was fully covered with mycelium of *P. chrysosporium* CK01 during the solid-state fermentation (SSF) process.

These remarkable enhancements in tensile strength can be attributed to several factors. Firstly, the fungus's enzymatic activity effectively removed non-cellulosic components (such as lignin, hemicellulose, wax, and pectin) and impurities from SCG biomass. This enzymatic action broke down complex molecules, altering their structure and composition, a phenomenon previously described by Sun et al. (2022) [58]. This "cleaning" process resulted in a rougher and enhanced surface area for TSCG, facilitating better interaction with the PHB/PLA matrix through mechanical interlocking, thereby enhancing stress transmission at the interface [64]. Secondly, TSCG demonstrated good dispersion within the matrix, coupled with improved phase compatibility, which contributed to enhanced adhesion. The homogeneity of biocomposites with TSCG was associated with higher carbohydrate content, which can influence the strength and stiffness of the resulting biocomposites, as indicated in Table 5. During SSF, the fungus developed and attached to the substrate surface, forming a network of branching hyphae known as mycelium (Fig. 14). This mycelium network on the SCG surfaces created an entangled structure, strengthening the interfacial connection between phases [58]. Fig. 15 further shows the changes of SCG throughout the biological treatment, after treated, the mycelium and the TSCG were mixed throughout and incubated at room temperatures for a specific period. This fungal treatment enhanced the biocomposite's ability to resist deformation and failure under tensile stress. The enhanced durability properties of TSCG-reinforced biocomposites can be attributed to the robust bonding between TSCG and the matrix, as evidenced by SEM micrographs (Fig. 11). TSCG particles are embedded in the matrix, indicating a continuous interfacial region between these two phases. Mechanical interlocking with the matrix facilitates this reactive reinforcing role, which explains why biocomposites with TSCG have increased mechanical strength. Furthermore, this observation is supported by the data presented in Table 7, which illustrates a reduction in void content, thereby minimising stress concentration points.

3.5.2. Tensile modulus

Fig. 16 presents the variation in tensile modulus of the biocomposites with different PHB/PLA ratios and SCG loadings. The tensile modulus exhibited an upward trend with increasing PLA content, with values ranging from 961.10 MPa for neat PHB to 1076.32 MPa for the PHB25/PLA75 blend. PLA has a higher initial modulus (1142.92 MPa) than PHB (961.10 MPa). This increase in modulus is mostly due to the inherent stiffness of PLA, which is in agreement with the findings of Ferreira et al. (2002) [65]. It can be noticed that excessive SCG can negatively affect the tensile modulus of PHB/PLA blends. A pronounced decrease was observed in biocomposites containing 40 wt% SCG (ranging from 688.75 to 1025.35 MPa) in contrast to those incorporating 10 wt% SCG (ranging from 976.78 to 1131.72 MPa). Interestingly, this outcome is contrary to previous studies that have suggested that the resistance of polymer composites to applied stress is directly proportional to filler loading [20,23,62]. The reduction in tensile modulus can be attributed to the "inhibition effect" of coffee oil present in SCG, which diminishes adhesion between SCG and the matrix [24]. This result finds similarities with the observations of Oksman et al. (2003) [66], who highlighted that an increase in reinforcement content did not guarantee a corresponding increase in the modulus of natural fiber-reinforced composites. This inconsistency might be due to fiber orientation during manufacturing, which can result in random alignment, affecting stiffness. Another explanation could be due to the homogeneity of filler dispersion [67]. Higher SCG contents tend to form agglomerates and struggle to disperse uniformly within the matrix, resulting in a lower tensile modulus.

Biological treatment had a positive impact on the tensile modulus of all TSCG-reinforced biocomposites (Fig. 17). It resulted in an increase ranging from 28 % to 34 % compared to their counterparts reinforced with USCG. The highest tensile modulus was achieved by PHB50/PLA50/TSCG20_PC55 biocomposite, reaching 1255.17 MPa. It was closely followed by PHB50/PLA50/TSCG20_AN50 biocomposite, which reached 1253.30 MPa, representing enhancements of 34 % and 33 %, respectively, when compared to PHB50/PLA50/SCG20 with a tensile modulus of 939.17 MPa. Notably, the biocomposite with the smallest incremental gain in tensile modulus was PHB50/PLA50/TSCG20_AN40, reaching 1201.15 MPa. This confirmed that the biological treatment contributed to improved interaction between TSCG and the PHB/PLA matrix, leading to better stress transfer at the biocomposite interface.

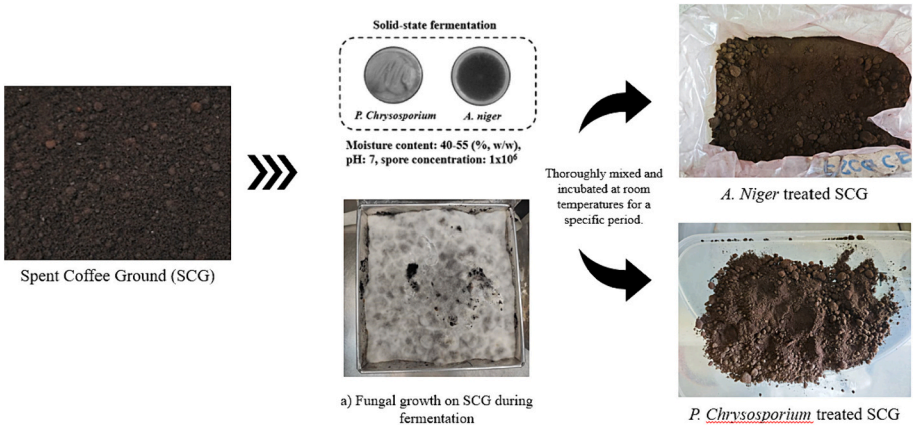

Fig. 15. Schematic of biological treatment of SCG (*P. chrysosporium and A. niger*). ; a) Appearance of SCG during the treatment.

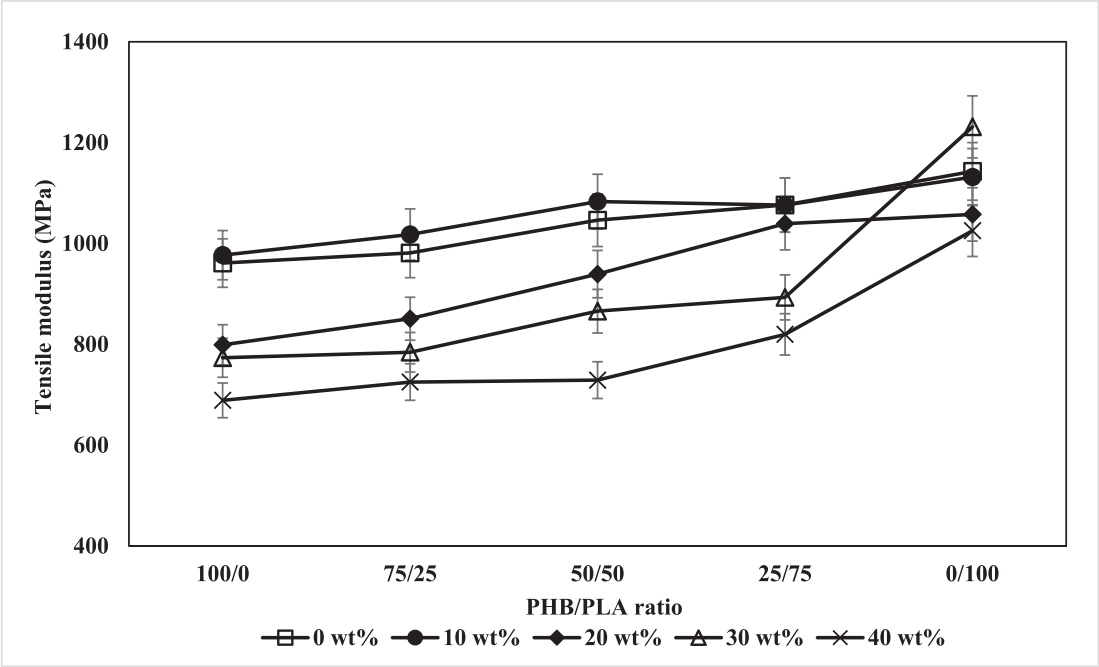

Fig. 16. Tensile modulus of PHB/PLA biocomposites with different combination of USCG and PHB/PLA matrix ratio.

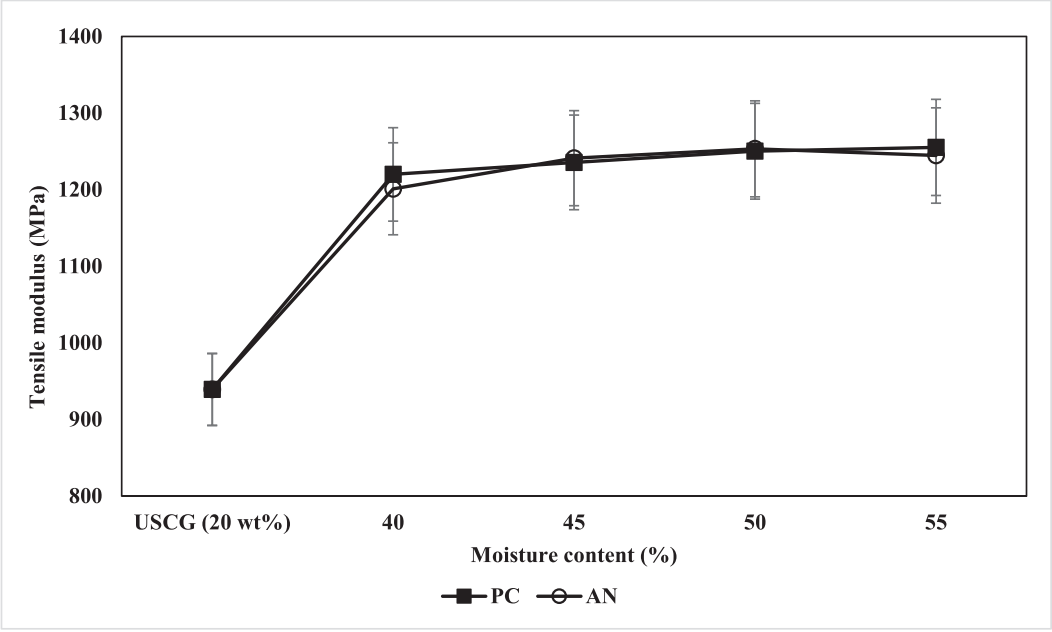

Fig. 17. Tensile modulus of PHB/PLA biocomposites with SCG treated at different moisture contents.

Another possible reason for this enhancement could be linked to the lower fat content of TSCG after the treatment process, which likely resulted in a more homogeneous dispersion of TSCG in the PHB/PLA matrix. These results resonate with those of Wu et al. (2016) [24], who observed that the extraction of coffee oil enhanced the interlocking between extracted SCG (ESCG) and PP, resulting in increased tensile modulus. Although it was previously discussed that PLA contributes to the strength of biocomposites, it is interesting to note that PHB50/PLA50/TSCG20 biocomposites showed even higher tensile modulus values, ranging from 1201.15 to 1255.17 MPa, compared to biocomposites with higher PLA content in PHB25/PLA75/SCG20, which had a tensile modulus of 1039.09 MPa. However, no significant effect was observed for the comparison between composites made of PC treated SCG and AN treated SCG.

3.5.3. *Tensile strain*

The study found that the tensile strain of the biocomposites gradually decreased from 5.65 % to 1.52 % with an increase in PLA ratio from 0 to 75 (Fig. 18). This decrease could be attributed to the inherent stiffness of PLA. The addition of SCG further reduced the strain values, ranging from 0.76 to 2.70 % and 0.05–2.36 % for biocomposites with 10 wt% and 40 wt% USCG, respectively. However, no significant trend was observed in tensile strains with varying SCG content. The stiffening effect arises from the reinforcing effect of rigid SCG, restricting the molecular

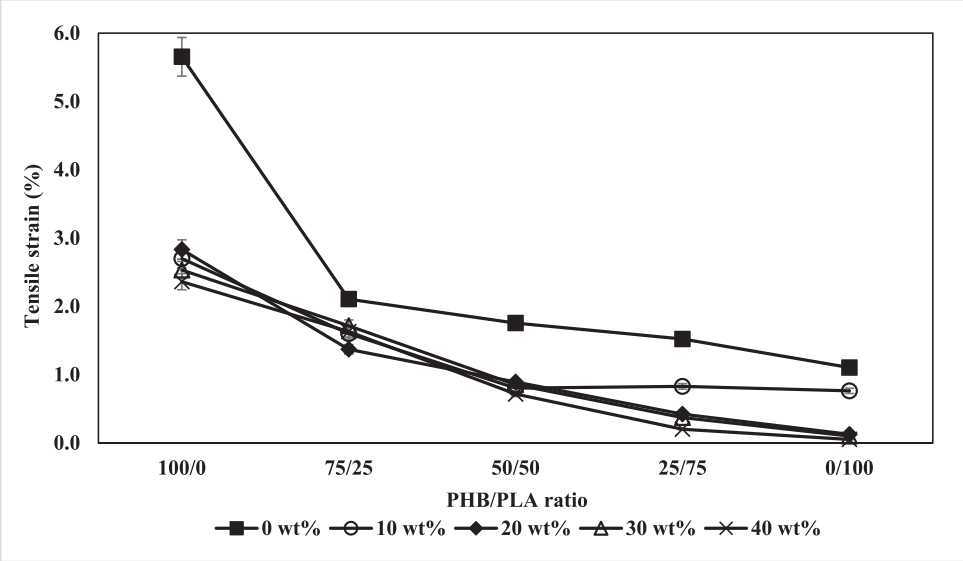

Fig. 18. Tensile strain of PHB/PLA biocomposites with different combination of USCG and PHB/PLA matrix ratio.

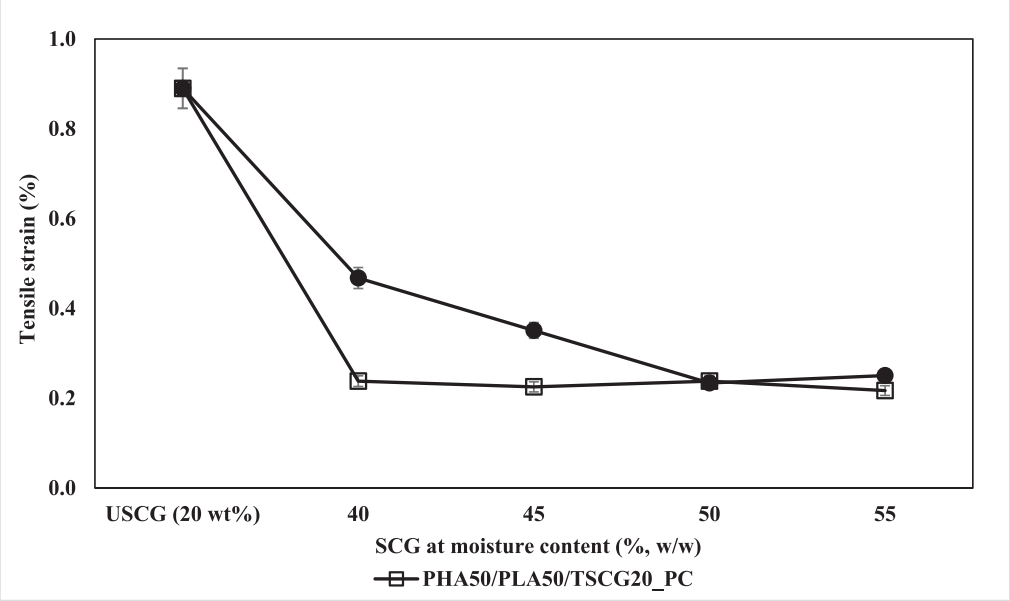

Fig. 19. Tensile strain of PHB/PLA biocomposites with SCG treated at different moisture contents.

mobility of the PHB/PLA matrix and making the biocomposite materials less stretchable [10,22]. These results are consistent with prior research indicating that tensile strain tends to decrease with the addition of various fillers [19,20,68].

The tensile strain of TSCG-reinforced PHB/PLA biocomposites before and after treatment was measured and compared (Fig. 19). The results revealed that the incorporation of TSCG did not increase the strain, but it exhibited slightly lower values (0.22 %–0.47 %), compared to the PHB50/PLA50/SCG20 biocomposite (0.89 %). No significant difference was observed among biocomposites with SCG treated at different moisture contents. This outcome could be explained by the restraining effect exerted by the stiffer TSCG on the movement of polymer chains [10]. As the stiffness of the biocomposites increased, the tensile strain decreased. The effectiveness of fungal treatment was proven by the enhanced interaction and mechanical interlocking between TSCG and the PHB/PLA matrix, yielding greater tensile characteristics within the biocomposites.

4. Conclusions

The study investigates the use of SCG as a reinforcement agent for PHB/PLA matrix and its impact on the mechanical and morphological properties of the resulting biocomposites. The hydrophilic nature of SCG is inherently incompatible with the hydrophobic properties of PHB and PLA, leading to compromised interfacial adhesion and inefficient stress transfer. Higher SCG content in the matrix induces particle agglomeration and creates stress concentration points. The presence of voids and gaps within the biocomposites further confirmed this incompatibility, resulting in decreased tensile properties. Factors such as SCG content, its dispersion characteristics, PHB/PLA ratio, and interfacial properties influence the tensile properties of biocomposites.

Biological treatment of SCG using *P. chrysosporium* CK01 and *A. niger* DWA8 resulted in increased carbohydrate, protein, crude fiber, and ash contents while decreasing fat and moisture levels. Enzyme activity was influenced by different moisture conditions, with *P. chrysosporium* CK01

showing maximum enzyme activity at 55 % (*w*/w) moisture content. In contrast, *A. niger* DWA8 displayed optimal growth at 40 % (w/w) moisture content, and the highest enzyme activity was observed at 55 %, 55 %, and 50 % (w/w) moisture content for CMCase, FPase, and MnP enzymes, respectively. The treatment also increased the surface roughness of SCG, promoting interaction between treated SCG and the matrix and improving the tensile properties of biocomposites. SEM micrographs confirmed the uniform dispersion of treated SCG within the matrix. This study proposes an environmentally friendly alternative for repurposing SCG generated by the coffee industry as a potential component for polymer composites. The enhanced comprehensive properties of PHB/PLA biocomposites with TSCG offer potential to replace conventional PLA products.

CRediT authorship contribution statement

J.Y. Boey: Formal analysis, Investigation, Visualization, Writing – original draft. **U. Kong:** Formal analysis, Investigation, Visualization, Writing – original draft. **C.K. Lee:** Conceptualization, Formal analysis, Investigation, Project administration, Supervision, Writing – review & editing. **G.K. Lim:** Writing – review & editing. **C.W. Oo:** Writing – review & editing. **C.K. Tan:** Writing – review & editing. **C.Y. Ng:** Writing – review & editing. **A.A. Azniwati:** Writing – review & editing. **G.S. Tay:** Conceptualization, Formal analysis, Funding acquisition, Investigation, Project administration, Supervision, Writing – review & editing.

Declaration of competing interest

The authors declare the following financial interests/personal relationships which may be considered as potential competing interests:

Tay Guan Seng reports financial support was provided by Universiti Sains Malaysia. Tay Guan Seng reports financial support and equipment, drugs, or supplies were provided by PMI Packaging Sdn. Bhd. Tay Guan Seng reports financial support and equipment, drugs, or supplies were provided by CY Enterprise Sdn. Bhd. If there are other authors, they declare that they have no known competing financial interests or personal relationships that could have appeared to influence the work reported in this paper.

Data availability

Data will be made available on request.

Acknowledgment

The authors would like to express their appreciation to Universiti Sains Malaysia for the funding support (1001/PTEKIND/8014123), PMI Packaging Sdn. Bhd., and CY Enterprise Sdn. Bhd. for the research materials supply (PLA, PHB, and spent coffee ground).

References

[1] K. Hamad, M. Kaseem, M. Ayyoob, J. Joo, F. Deri, Polylactic acid blends: the future of green, light and tough, Prog. Polym. Sci. 85 (2018) 83–127, https://doi.org/10.1016/j. progpolymsci.2018.07.001.
[2] M. Zwawi, A review on natural Fiber bio-composites, surface modifications and applications, Molecules 26 (2021) 404, https://doi.org/10.3390/molecules26020404.
[3] T. Narancic, F. Cerrone, N. Beagan, K.E. O'Connor, Recent advances in bioplastics: application and biodegradation, Polymers 12 (2020), https://doi.org/10.3390/POLYM12040920.
[4] C. Nielsen, A. Rahman, A.U. Rehman, M.K. Walsh, C.D. Miller, Food waste conversion to microbial polyhydroxyalkanoates, J. Microbial. Biotechnol. 10 (2017) 1338–1352, https://doi.org/10.1111/1751-7915.12776.
[5] N.C. Loureiro, J.L. Esteves, J.C. Viana, S. Ghosh, Development of polyhydroxyalkanoates/poly(lactic acid) composites reinforced with cellulosic fibers, Compos. Part B Eng. 60 (2014) 603–611, https://doi.org/10.1016/J.COMPOSITESB.2014.01.001.
[6] O. Olejnik, A. Masek, J. Zawadziłło, Processability and mechanical properties of thermoplastic Polylactide/Polyhydroxybutyrate (PLA/PHB) bioblends, Materials 14 (2021) 898, https://doi.org/10.3390/ma14040898.
[7] M.I.N. Zhang, N.L. Thomas, Blending polylactic acid with polyhydroxybutyrate: the effect on thermal, mechanical, and biodegradation properties, Advances in Po 30 (2011) 67–79, https://doi.org/10.1002/adv.
[8] H. Moustafa, C. Guizani, A. Dufresne, Sustainable biodegradable coffee grounds filler and its effect on the hydrophobicity, mechanical and thermal properties of biodegradable PBAT composites, Journal of Applied Polymer Science 134 (2016), https://doi.org/10.1002/APP.44 498.
[9] D.K. Rajak, D.D. Pagar, P.L. Menezes, E. Linul, Fiber-reinforced polymer composites: manufacturing, properties, and applications, Polymers 11 (2019) doi: 10.3390/POLYM11101667.
[10] G. Gaidukova, O. Platnieks, A. Aunins, A. Barkane, C. Ingrao, S. Gaidukovs, Spent coffee waste as a renewable source for the production of sustainable poly(butylene succinate) biocomposites from a circular economy perspective, RSC Adv. 11 (2021) 18580–18589, https://doi.org/10.1039/D1RA03203H.
[11] P. Tapangnoi, P. Sae-Oui, W. Naebpetch, C. Siriwong, Preparation of purified spent coffee ground and its reinforcement in natural rubber composite, Arab. J. Chem. 15 (2022) 103917, https://doi.org/10.1016/j.arabjc.2022.103917.
[12] P.S. Murthy, M. Madhava Naidu, Sustainable management of coffee industry by-products and value addition - a review, Resour. Conserv. Recycl. 66 (2012) 45–58, https://doi.org/10.1016/j.resconrec.2012.06.005.
[13] X.-E. Chen, D. Mangindaan, H.-W. Chien, Green sustainable photothermal materials by spent coffee grounds, J. Taiwan Inst. Chem. Eng. 137 (2022) 104259, https://doi.org/10.1016/j.jtice.2022.104259.
[14] P.-C. Hsieh, Y.-C. Chen, N.-C. Zheng, D. Mangindaan, H.-W. Chien, A low-cost and environmentally-friendly chitosan/spent coffee grounds composite with high photothermal properties for interfacial water evaporation, J. Ind. Eng. Chem. 126 (2023) 283–291, https://doi.org/10.1016/j.jiec.2023.06.019.
[15] G. Dattatraya Saratale, R. Bhosale, S. Shobana, J.R. Banu, A. Pugazhendhi, E. Mahmoud, R. Sirohi, S. Kant Bhatia, A.E. Atabani, V. Mulone, J.-J. Yoon, H. Seung Shin, G. Kumar, A review on valorization of spent coffee grounds (SCG) towards biopolymers and biocatalysts production, Bioresour. Technol. 314 (2020) 123800, https://doi.org/10.1016/j.biortech.2020.123800.
[16] A. Bomfim, D. Oliveira, H. Voorwald, K. Benini, M.-J. Dumont, D. Rodrigue, Valorization of spent coffee grounds as precursors for biopolymers and composite production, Polymers 14 (2022) 437, https://doi.org/10.3390/polym14030437.
[17] T.A. Nguyen, Q.T. Nguyen, Hybrid biocomposites based on used coffee grounds and epoxy resin: mechanical properties and fire resistance, Int. J. Chem. Eng. 2021 (2021) 1–12, https://doi.org/10.1155/2021/1919344.
[18] N.M. Nurazzi, M.M. Harussani, H.A. Aisyah, R.A. Ilyas, M.N.F. Norrrahim, A. Khalina, N. Abdullah, Treatments of natural fiber as reinforcement in polymer composites—a short review, Functional Composites and Structures 3 (2021) 024002, https://doi.org/10.1088/2631-6331/ABFF36.
[19] M. George, P.G. Mussone, K. Alemaskin, M. Chae, J. Wolodko, D.C. Bressler, Enzymatically treated natural fibres as reinforcing agents for biocomposite material: mechanical, thermal, and moisture absorption characterization, J. Mater. Sci. 51 (2015) 2677–2686, https://doi.org/10.1007/s10853-015-9582-z.
[20] L.Y. Jaramillo, M. Vásquez-Rendón, S. Upegui, J.C. Posada, M. Romero-Sáez, Polyethylene-coffee husk eco-composites for production of value-added consumer products, Sustain Environ Res 31 (2021) 34, https://doi.org/10.1186/s42834-021-00107-6.
[21] O.J. Shesan, A.C. Stephen, A.G. Chioma, R. Neerish, S.E. Rotimi, Improving the mechanical properties of natural fiber composites for structural and biomedical applications, in: A.B. Pereira, F.A.O. Fernandes (Eds.), Renewable and Sustainable Composites, IntechOpen, 2019, https://doi.org/10.5772/intechopen.85252.
[22] H. Essabir, M. Raji, S.A. Laaziz, D. Rodrique, R. Bouhfid, A. El Kacem Qaiss, Thermo-mechanical performances of polypropylene biocomposites based on untreated, treated and compatibilized spent coffee grounds, Composites Part B: Engineering 149 (2018) 1–11, https://doi.org/10.1016/j.compositesb.2018.05.020.
[23] Z.C. Lule, J. Kim, Properties of economical and eco-friendly polybutylene adipate terephthalate composites loaded with surface treated coffee husk, Compos. A: Appl. Sci. Manuf. 140 (2021) 106154, https://doi.org/10.1016/j.compositesa.2020.106154.
[24] H. Wu, W. Hu, Y. Zhang, L. Huang, J. Zhang, S. Tan, X. Cai, X. Liao, Effect of oil extraction on properties of spent coffee ground–plastic composites, J. Mater. Sci. 51 (2016) 10205–10214, https://doi.org/10.1007/s10853-016-0248-2.
[25] NatureWorks, Ingeo™ Biopolymer 2003D Technical Data Sheet, (n.d.).
[26] Biobased Pha Biodegradable Resin for Mulch Film, (n.d.). https://ecomann.en.made-in-china.com/product/qvLmVkKHZgcl/China-Biobased-Pha-Biodegradable-Resin-for-Mulch-Film.html (accessed September 1, 2023).
[27] P.K. Pang, I. Darah, L. Poppe, G. Szakacs, C.O. Ibrahim, Xylanase production by a local isolate, Trichoderma spp. FETL c3–2 via solid state fermentation using agricultural wastes as substrates, MJM (2006), https://doi.org/10.21161/mjm.210602.
[28] A. Gessesse, G. Mamo, High-level xylanase production by an alkaliphilic Bacillus sp. by using solid-state fermentation, Enzyme Microb. Technol. 25 (1999) 68–72, https://doi.org/10.1016/S0141-0229(99)00006-X.
[29] T.K. Ghose, Measurement of cellulase activities, Pure Appl. Chem. 59 (1987) 257–268, https://doi.org/10.1351/PAC198759020257.
[30] M.L.C. Silva, V.B.D. Souza, V.D.S. Santos, H.M. Kamida, J.R.T.D. Vasconcellos-Neto, A. Góes-Neto, M.G. Bello Koblitz, Production of manganese peroxidase by Trametes villosa on Unexpensive substrate and its application in the removal of

lignin from agricultural wastes, ABB 05 (2014) 1067–1077, https://doi.org/10.4236/abb.2014.514122.
[31] M.J. Swift, The estimation of mycelial biomass by determination of the hexosamine content of wood tissue decayed by fungi, Soil Biol. Biochem. 5 (1972) 321–332, https://doi.org/10.1016/0038-0717(73)90080-1.
[32] AOAC International, Official Methods of Analysis of AOAC International, 2012.
[33] ASTM D2734-94, Standard Test Methods for Void Content of Reinforced Plastics, 2003.
[34] ASTM D638-14, Standard Test Method for Tensile Properties of Plastics, 2014.
[35] Z.K. Terefe, M.N. Omwamba, J.M. Nduko, Effect of solid state fermentation on proximate composition, antinutritional factors and in vitro protein digestibility of maize flour, Food Sci. Nutr. 9 (2021) 6343–6352, https://doi.org/10.1002/fsn3.2599.
[36] J.B. Ulloa Rojas, J.A.J. Verreth, S. Amato, E.A. Huisman, Biological treatments affect the chemical composition of coffee pulp, Bioresour. Technol. 89 (2003) 267–274, https://doi.org/10.1016/S0960-8524(03)00070-1.
[37] Y. Pranoto, S. Anggrahini, Z. Efendi, Effect of natural and lactobacillus plantarum fermentation on in-vitro protein and starch digestibilities of sorghum flour, Food Biosci. 2 (2013) 46–52, https://doi.org/10.1016/j.fbio.2013.04.001.
[38] O.O. Olukomaiya, O.Q. Adiamo, W.C. Fernando, R. Mereddy, X. Li, Y. Sultanbawa, Effect of solid-state fermentation on proximate composition, anti-nutritional factor, microbiological and functional properties of lupin flour, Food Chem. 315 (2020) 126238, https://doi.org/10.1016/j.foodchem.2020.126238.
[39] P.O. Uvere, E.U. Onyekwere, P.O. Ngoddy, Production of maize-bambara groundnut complementary foods fortified pre-fermentation with processed foods rich in calcium, iron, zinc and provitamin a: pre-fermentation fortified maize-bambara infant foods, J. Sci. Food Agric. 90 (2010) 566–573, https://doi.org/10.1002/jsfa.3846.
[40] S. Obruca, S. Petrik, P. Benesova, Z. Svoboda, L. Eremka, I. Marova, Utilization of oil extracted from spent coffee grounds for sustainable production of polyhydroxyalka- noates, Appl. Microbiol. Biotechnol. 98 (2014) 5883–5890, https://doi.org/10.1007/s 00253-014-5653-3.
[41] S. Saithi, A. Tongta, Phytase production of aspergillus Niger on soybean meal by solid-state fermentation using a rotating drum bioreactor, Agriculture and Agricultural Science Procedia 11 (2016) 25–30, https://doi.org/10.1016/j.aaspro.2016.12.005.
[42] G.D. Saratale, S.D. Kshirsagar, V.T. Sampange, R.G. Saratale, S.-E. Oh, S. P. Govindwar, M.-K. Oh, Cellulolytic enzymes production by utilizing agricultural wastes under solid state fermentation and its application for biohydrogen production, Appl. Biochem. Biotechnol. 174 (2014) 2801–2817, https://doi.org/10.1007/s12010-014-1227-1.
[43] L.W. Yoon, G.C. Ngoh, A.S.M. Chua, M.F. Abdul Patah, W.H. Teoh, Process intensification of cellulase and bioethanol production from sugarcane bagasse via an integrated saccharification and fermentation process, Chemical Engineering and Processing-Process Intensification 142 (2019) 107528, https://doi.org/10.1016/j.cep.2019.107528.
[44] R.J.S. De Castro, H.H. Sato, Enzyme production by solid state fermentation: general aspects and an analysis of the physicochemical characteristics of substrates for agro-industrial wastes valorization, Waste Biomass Valor 6 (2015) 1085–1093, https://doi.org/10.1007/s 12649-015-9396-x.
[45] J.J. Abdullah, D. Greetham, Optimizing cellulase production from municipal solid waste (MSW) using solid state fermentation (SSF), J Fundam Renewable Energy 6 (2016), https://doi.org/10.4172/2090-4541.1000206.
[46] G.S. Anisha, R.K. Sukumaran, P. Prema, Evaluation of α-galactosidase biosynthesis by Streptomyces griseoloalbus in solid-state fermentation using response surface methodo- logy, Lett. Appl. Microbiol. 46 (2008) 338–343, https://doi.org/10.1111/j.1472-765X.2008.02321.x.
[47] L.W. Yoon, T.N. Ang, G.C. Ngoh, A.S.M. Chua, Fungal solid-state fermentation and various methods of enhancement in cellulase production, Biomass Bioenergy 67 (2014) 319–338, https://doi.org/10.1016/j.biombioe.2014.05.013.
[48] M. Ramzan, M. Asgher, M.A. Sheikh, H.N. Bhatti, Hyperproduction of manganese peroxidase through chemical mutagenesis of trametes versicolor IBL-04 and optimization of process parameters, BioResources 8 (2013) 3953–3966, doi: 10.15376/biores.8.3.3953-3966.
[49] N. Vassilev, A.R. Requena, L.M. Nieto, I. Nikolaeva, M. Vassileva, Production of manganese peroxidase by Phanerochaete chrisosporium grown on medium containing agro-wastes/rock phosphate and biocontrol properties of the final product, Industrial Crops and Products 30 (2009) 28–32, https://doi.org/10.1016/j.indcrop.2009.01.001.
[50] N. Darabzadeh, Z. Hamidi-Esfahani, P. Hejazi, Optimization of cellulase production under solid-state fermentation by a new mutant strain of *Trichoderma reesei*, Food Sci. Nutr. 7 (2019) 572–578, https://doi.org/10.1002/fsn3.852.
[51] N. Nadir, N.L. Ismail, A.S. Hussain, Fungal pretreatment of lignocellulosic materials, Biomass for Bioenergy-Recent Trends and Future Challenges (2019) doi: 10.5772/INTECHOPEN.84239.
[52] S.B. Carter, S.E. Nokes, C.L. Crofcheck, The influence of environmental temperature and substrate initial moisture content on Aspergillus niger growth and phytase production in solid-state cultivation, Transactions of the ASAE 47 (2004) 945–949, https://doi.org/10.13031/2013.16073.
[53] V. Sharma, M.L. Meena, M. Kumar, Effect of filler percentage on physical and mechanical characteristics of basalt fiber reinforced epoxy based composites, Materials Today: Proceedings 26 (2020) 2506–2510, https://doi.org/10.1016/j.matpr.2020.02.533.
[54] X. Xu, Z. Xu, S. Shi, M. Lin, Lignocellulose degradation patterns, structural changes, and enzyme secretion by Inonotus obliquus on straw biomass under submerged fermentation, Bioresour. Technol. 241 (2017) 415–423, https://doi.org/10.1016/j.biortech. 2017.05.087.
[55] G. Zhuo, X. Zhang, X. Jin, M. Wang, X. Yang, S. Li, Effect of different enzymatic treatment on mechanical, water absorption and thermal properties of bamboo fibers reinforced poly(Hydroxybutyrate-co-Valerate) biocomposites, J. Polym. Environ. 28 (2020) 2377–2385, https://doi.org/10.1007/S10924-020-01781-0.
[56] K.L. Pickering, M.G.A. Efendy, T.M. Le, A review of recent developments in natural fibre composites and their mechanical performance, Compos. A: Appl. Sci. Manuf. 83 (2016) 98–112, https://doi.org/10.1016/j.compositesa.2015.08.038.
[57] K.J. Vishnu Vardhini, R. Murugan, R. Surjit, Effect of alkali and enzymatic treatments of banana fibre on properties of banana/polypropylene composites, J. Ind. Text. 47 (2018) 1849–1864, https://doi.org/10.1177/1528083717714479.
[58] W. Sun, M. Tajvidi, C.G. Hunt, B.J.W. Cole, C. Howell, D.J. Gardner, J. Wang, Fungal and enzymatic pretreatments in hot-pressed lignocellulosic bio-composites: a critical review, J. Clean. Prod. 353 (2022) 131659, https://doi.org/10.1016/j.jclepro. 2022.131659.
[59] D. Aydemir, D.J. Gardner, Biopolymer blends of polyhydroxybutyrate and polylactic acid reinforced with cellulose nanofibrils, Carbohydrate Polymers (2020) 116867, https://doi.org/10.1016/j.carbpol.2020.116867.
[60] C.H. Lee, A. Khalina, S.H. Lee, Importance of interfacial adhesion condition on characterization of plant-Fiber-reinforced polymer composites: a review, Polymers 13 (2021) 438, https://doi.org/10.3390/POLYM13030438.
[61] B.S. Baek, J.W. Park, B.H. Lee, H.J. Kim, Development and application of green composites: using coffee ground and bamboo flour, J. Polym. Environ. 21 (2013) 702–709, https://doi.org/10.1007/s10924-013-0581-3.
[62] G. Totaro, L. Sisti, M. Fiorini, I. Lancellotti, F.N. Andreola, A. Saccani, Formulation of green particulate Composites from PLA and PBS matrix and wastes deriving from the coffee production, J. Polym. Environ. 27 (2019) 1488–1496, https://doi.org/10.1007/s10924-019-01447-6.
[63] M.A. Gunning, L.M. Geever, J.A. Killion, J.G. Lyons, C.L. Higginbotham, Mechanical and biodegradation performance of short natural fibre polyhydroxybutyrate composites, Polym. Test. 32 (2013) 1603–1611, https://doi.org/10.1016/j.polymertesting.2013.10.011.
[64] S.M. Khoshnava, R. Rostami, M. Ismai, A. Valipour, The using fungi treatment as green and environmentally process for surface modification of natural fibres, Applied Mechanics and Materials 554 (2014) 116–122, https://doi.org/10.4028/www.scientific.net/AMM.554.116.
[65] B.M.P. Ferreira, C.A.C. Zavaglia, E.A.R. Duek, Films of PLLA/PHBV: thermal, morphological, and mechanical characterization, J. Appl. Polym. Sci. 86 (2002) 2898–2906, https://doi.org/10.1002/app.11334.
[66] K. Oksman, M. Skrifvars, J.-F. Selin, Natural fibres as reinforcement in polylactic acid (PLA) composites, Composites Science and Technology 63 (2003) 1317–1324, doi:10. 1016/S0266-3538(03)00103-9.
[67] N.I. Ismail, Z.A.M. Ishak, Effect of fiber loading on mechanical and water absorption capacity of polylactic acid/polyhydroxybutyrate-co-hydroxyhexanoate/Kenaf composite, IOP Conf. Ser.: Mater. Sci. Eng. 368 (2018) 012014, https://doi.org/10.1088/1757-899X/368/1/012014.
[68] R. Chaari, M. Khlif, H. Mallek, C. Bradai, C. Lacoste, H. Belguith, H. Tounsi, P. Dony, Enzymatic treatments effect on the poly (butylene succinate)/date palm fibers properties for bio-composite applications, Ind. Crop. Prod. 148 (2020) 112270, https://doi.org/10.1016/j.indcrop.2020.112270.